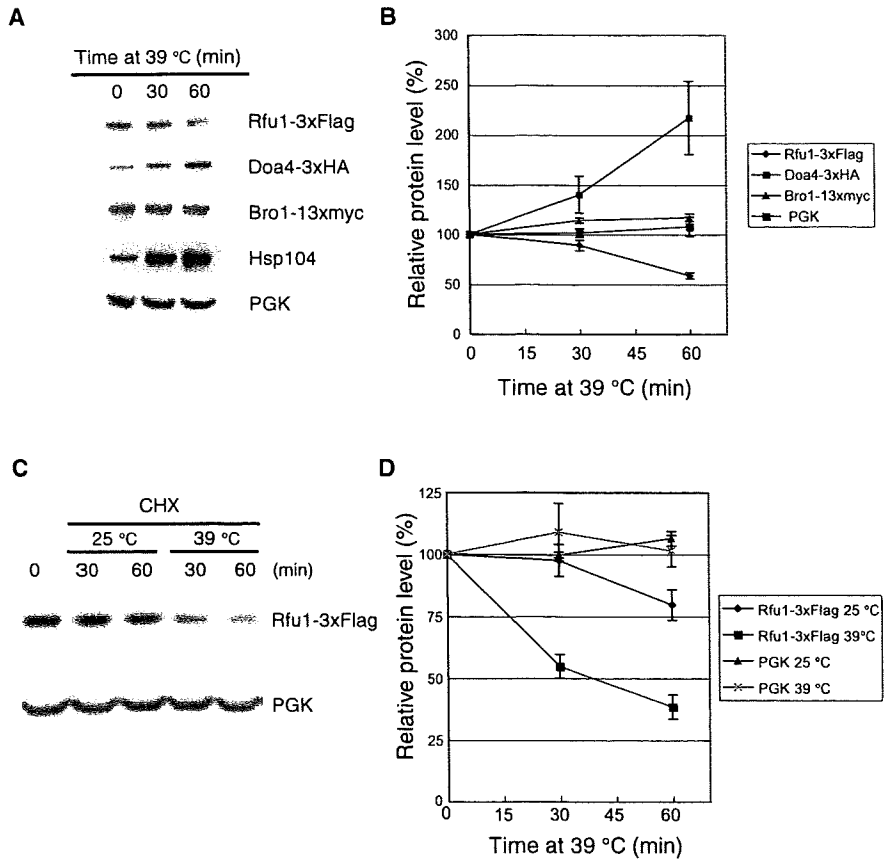

Figure 5. Rfu1-3×Flag, Doa4-3×HA, and Bro1-13×myc Protein Levels in Response to Heat Shock

(A) Rfu1-3×Flag, Doa4-3×HA, Bro1-13×myc, and PGK protein levels under heat shock at 39°C. Total cell lysates obtained at the indicated time points were analyzed by immunoblotting with anti-Flag, anti-HA, anti-myc, anti-Hsp104, and anti-PGK.

(B) Quantification of protein levels. Protein levels were quantified from the bands shown in (A). Data are mean ± SEM values of three independent experiments.

(C) Rfu1-3×flag and PGK protein levels under heat shock in the presence of cycloheximide.

(D) Quantification of protein levels. Protein levels were quantified from the bands shown in (C). Data are mean ± SEM values of three independent experiments.

mammalian cultured cells (Carlson et al., 1987). The heat treatment also resulted in marked increase in Hsp104 protein, one of the major heat-inducible proteins. Surprisingly, heat treatment resulted in disappearance of free Ub chains; their level decreased after 15 min of such treatment.

We speculated that one reason for the marked decrease in free Ub chains upon heat treatment was the disassembling of free Ub chains by certain DUBs to produce more monomeric Ub, which can be used for ubiquitination reactions. Accordingly, we examined the involvement of DUB activity in stress-induced disappearance of free Ub chains. Ub(G76A), in which the last amino acid of glycine in Ub is replaced with alanine, is reported to form a Ub chain, but it is resistant to the action of deubiquitinating enzymes (Hodgins et al., 1992). Plasmids expressing G76A monomeric Ub or wild-type monomeric Ub under the regulation of Cup1 promoter were introduced into wild-type cells (Figure 4B). In the absence of copper, when essentially only endogenous Ub-encoding genes were expressed, heat treatment markedly decreased the level of free Ub chains. Copper-induced exogenous wild-type Ub expression increased free Ub chains but decreased the chains upon heat shock. On the other hand, in cells expressing Ub(G76A), heat shock did not reduce the amount of small Ub oligomer-like species. Although we cannot exclude the possibility that the observed results are due to reasons other than that UbG76A is a poor substrate for DUBs, the above findings emphasize the potential involvement of DUB(s) in the disappearance of free Ub chains.

We further investigated whether Doa4 mediates the heat shock-induced decrease in free Ub chains. To test this, *Δdoa4* cells were heat shocked and the Ub profiles of the cells were examined. Compared with wild-type cells, substantial amounts of free Ub chains remained in *Δdoa4* cells even after 1 hr of heat shock (Figure 4C), suggesting the involvement of Doa4 in this process. Next, we examined the effect of 3×HA-Rfu1 overexpression. If Rfu1 inhibits Doa4, overexpression of 3×HA-Rfu1 should phenocopy *Δdoa4* mutant with respect to heat shock-induced disappearance of free Ub chains. Wild-type cells overexpressing 3×HA-Rfu1 were heat shocked, and the change in free Ub chains was examined. We found that overexpression of 3×HA-Rfu1 under the regulation of the glyceraldehyde-3-phosphate dehydrogenase (GPD) promoter significantly inhibited the disappearance of free Ub chains (Figures 4D and 4E). These results indicate that disappearance of free Ub chains is at least partly mediated by a balance of the actions of Doa4 and Rfu1.

Since the mRNA levels of *RFU1* and *DOA4* decrease and increase upon heat shock, respectively (Gasch et al., 2000), we decided to examine the effects of heat shock on the levels of their proteins. We found that the changes in Rfu1-3×Flag and Doa4-3×HA levels paralleled the reported changes in their mRNA levels upon heat treatment (Figures 5A and 5B). The amount of Rfu1-3×Flag decreased by 40%–50% after 60 min of heat shock. In contrast, heat shock increased the Doa4-3×HA level, though the increase was modest compared with the marked increase in the heat shock protein Hsp104. The level of Bro1-13×myc remained unchanged upon heat shock. These results were consistent with the notion that heat shock produces more Doa4 that is uninhibited by Rfu1and can thus contribute to disassembling free Ub chains.

We also tested whether decrease of Rfu1-3×Flag was also mediated at the protein level and thus examined the stability of Rfu-3×Flag. In cells treated with cycloheximide followed

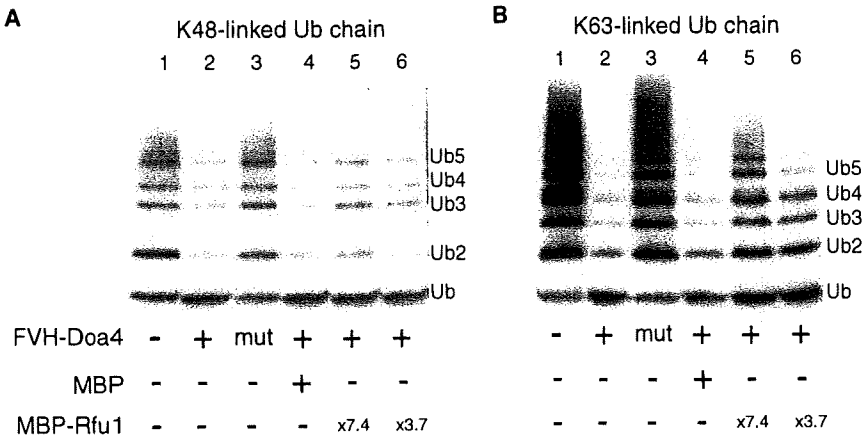

Figure 6. In Vitro Doa4 DUB Activity toward Ub Chains and Rfu1 Inhibition

(A and B) Detection of Doa4 DUB activity toward K48- or K63-linked Ub chains and inhibition by MBP-Rfu1. FVH-Doa4 (1.1 μg) and FVH-Doa4 (Cys571Ser) were added in lanes 2 and 3, respectively. MBP was added at 9.4-fold molar excess and MBP-Rfu1 was added at 7.4- and 3.7-fold molar excess to FVH-Doa4 (lanes 4, 5, and 6, respectively).

immediately by heat shock, Rfu1-3×Flag was rather stable at 25°C but became unstable upon heat shock (Figures 5C and 5D). This result indicated that the expression of Rfu1 is regulated both at mRNA and protein levels upon thermal stress.

Rfu1 Is an Inhibitor of Doa4 In Vitro

The above results suggested that Doa4 can disassemble free Ub chains to monomeric Ub, and that Rfu1 inhibits this activity. Next, we examined whether Doa4 can disassemble free Ub chains in vitro. We used K48-linked and K63-linked Ub chains as substrates because the linkage of Ub dimer purified from *Arabiodopsis* is Lys48-linked, and the linkage of free Ub chains purified from yeast expressing His-tagged Ub is mainly Lys48-linked, though also to some extent Lys63-linked (van Nocker and Vierstra, 1993; Xu and Peng, 2008). When FVH-Doa4 was incubated with K48-linked or K63-linked Ub chains, DUB activity was observed for K48-linked and, more effectively, for K63-linked Ub chains (Figures 6A and 6B, lane 2). These DUB activities were abolished with the catalytic mutant of Doa4 (Cys571Ser) (lane 3) (Papa and Hochstrasser, 1993). In the next experiment, we premixed MBP-Rfu1 or MBP with FVH-Doa4 and added K48- or K63-linked Ub chains to see whether MBP-Rfu1 has any inhibitory effect. The addition of MBP-Rfu1 markedly inhibited DUB activity for both K48- and K63-linked Ub chains in a dose-dependent manner (lanes 5 and 6). The inhibitory effect was not observed with MBP (lane 4). To test whether the inhibitory effect was specific to Doa4 (Figure S10), we purified a tagged Ubp14 (FVH-Ubp14) and its catalytic mutant FVH-Ubp14(Cys332Ser). FVH-Ubp14 showed very strong DUB activity toward Ub chains. The use of MBP-Rfu1 showed no inhibitory effect, indicating that the inhibitory effect of Rfu1 is specific to Doa4.

Since Rfu1 binds Bro1 in vivo (Figure 3D), it is possible that Rfu1-Bro1 complexes may be a contaminant in these experiments that inhibit FVH-Doa4. To exclude this possibility, we purified FVH-Doa4 from *Δbro1Δdoa4Δpep4* cells and retested in vitro assays with the FVH-Doa4. The FVH-Doa4 from *Δbro1 Δdoa4Δpep4* cells bound to MBP-Rfu1 and inhibited Doa4 DUB activity (Figure S11). These results indicate that Rfu1 directly inhibits the DUB activity of Doa4 in vitro.

DISCUSSION

Ub is used in numerous critical cellular events whereas monomeric Ub must be maintained at an adequate level at all times in response to different cellular conditions. Cells are equipped with defined systems to regulate monomeric Ub level (Finley et al., 1987; Hanna et al., 2007). Our analyses and results revealed a mechanism that regulates and maintains Ub levels; the balance of activities of DUB and its regulators determines the level of monomeric Ub. We propose that unanchored Ub chains function as a reservoir for monomeric Ub, as illustrated in Figure 7.

Rfu1 as an Inhibitor of Doa4

Based on the genetic and biochemical evidence provided in this study, we conclude that Rfu1 functions as an inhibitor of Doa4. Although several activators/inhibitors of DUBs have been reported (Ventii and Wilkinson, 2008), Rfu1 appears to provide the first example of inhibition of DUB both in vivo and in vitro. Since Doa4 functions in various important events, it is likely important to regulate Doa4 activity appropriately. Indeed, since Bro1 is an activator of Doa4 (Luhtala and Odorizzi, 2004; Richter et al., 2007), Doa4 is regulated by both an activator and an inhibitor. The exact molecular mechanism of Rfu1-induced Doa4 inhibition remains to be clarified, and this will elucidate how Rfu1 and Bro1 coordinate to regulate Doa4 activity. Bro1 recruits Doa4 through the interaction of the N-terminal noncatalytic region of Doa4, and Bro1 stimulates the deubiquitination activity of Doa4 through the interaction of the C-terminal catalytic region (Richter et al., 2007). For Doa4 to exhibit its function, it is important that it localizes in the endosome, a process dependent on Bro1 (Amerik et al., 2006; Richter et al., 2007). Based on the finding that Bro1 binds to Rfu1 in the absence of Doa4, we speculate that Bro1 also recruits Rfu1 to the endosome. Indeed, the localization of Rfu1-GFP in the endosome was largely lost in the *Δbro1* mutant (Y.K. and K.T., unpublished data). Preliminary experiments provided evidence against any role for Rfu1 in recruiting Doa4 to the endosomes; Doa4-GFP localization remained unchanged following the introduction of *Δrfu1* mutation in the *Δvps4* mutant (Y.K. and K.T., unpublished data). These results, together with the present observation of direct inhibition of Doa4 by Rfu1 in vitro (Figure 6), indicate that Rfu1 could act on Doa4 to inhibit its activity after Bro1 recruits Doa4 to the endosome. Indeed, Bro1 is about 25-fold more abundant than Doa4 and Rfu1 (Ghaemmaghami et al., 2003) and hence potentially has many roles in the cell. It should be noted that we cannot

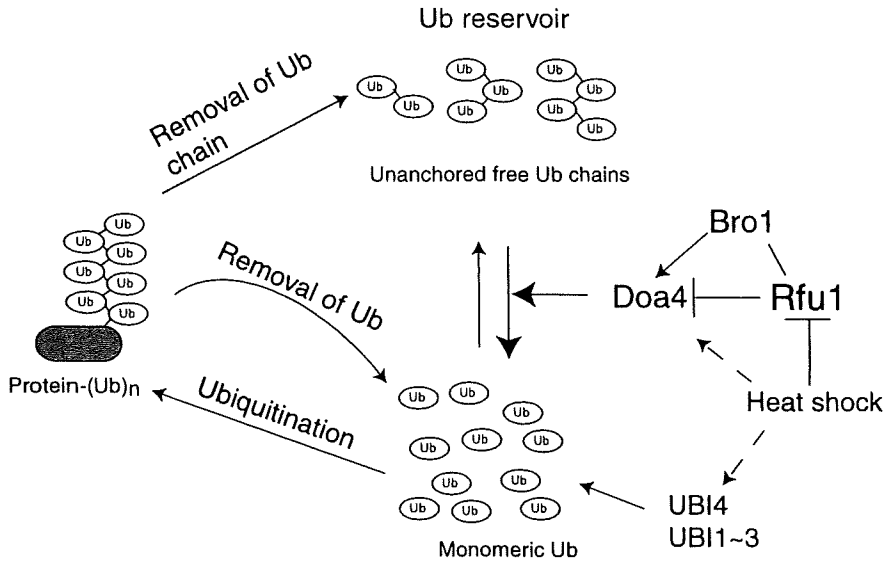

Figure 7. A Model of Regulation of Ub Homeostasis by Free Ub Chains

The monomeric ubiquitin (Ub) pool is maintained through synthesis from Ub-encoding genes, *UBI1–4*, by release from protein-conjugated Ub chains, and by release from free Ub chains. DUB(s), such as Doa4, supply monomeric Ub by cleaving free Ub chains. Under normal conditions, Rfu1 inhibits the activity of Doa4, resulting in the maintenance of the monomeric Ub pool, and consequently enhances the formation of free Ub chains. Upon heat shock, Rfu1 levels decrease and more Doa4 is produced (Figures 5A and 5B); therefore, monomeric Ub would be produced from free Ub chains by Doa4. In addition, transcription of *UBI4*-encoding polyubiquitin is increased. Since the activity of Doa4 is enhanced by Bro1, Doa4 would be controlled by a balance between its activator (e.g., Bro1) and inhibitor (e.g., Rfu1). Note that Bro1 is physically associated with Rfu1 (for details, see text).

exclude other functions for Rfu1 such as inhibition of Bro1 activity.

Rfu1 does not have any orthologs in higher eukaryotes. However, it has low sequence similarity to two different mammalian DUBs: AMSH and UBPY. The homologous regions lie mainly outside of the catalytic domains. Given that the homologous sequence is involved in the inhibition activity, the corresponding regions of AMSH and UBPY may also inhibit other DUBs or their own DUB activity.

Free Ub Chains, Doa4, Rfu1, and Heat Shock

More Ubs are required upon stress, probably due to the massive need of ubiquitination to degrade denatured proteins by the 26S proteasome (Finley et al., 1987). We showed that heat shock markedly decreased the levels of free Ub chains. We believe that production of monomeric Ub is regulated through deubiquitination activities and that heat stress increases monomeric Ub production by disassembling free Ub chains. Doa4 and Rfu1 are involved, even only in part, in this regulation, based on the following observations. First, Ub chains derived from Ub(G76A) remained after heat shock, suggesting the involvement of deubiquitination in the decrease of free Ub chains (Figure 4B). Second, overproduction of Doa4 into wild-type cells increased monomeric Ubs and decreased unanchored Ub chains (Figure S8), suggesting that Doa4 disassembles free Ub chains in vivo. Third, Doa4 indeed disassembled free Ub chains in vitro (Figure 6). Fourth, in Δ*doa4* mutant and wild-type cells overexpressing 3×HA-Rfu1, free Ub chains partly remained upon heat shock (Figures 4C–4E). Fifth, heat shock decreased Rfu1 and increased Doa4 protein levels (Figure 5A). However, in addition to Doa4, another DUB(s) may contribute to the disappearance of free Ub chains upon heat shock since the effects of *Δdoa4* mutation and Rfu1 overexpression were far from complete. DUBs whose mutants show altered Ub profile may be good candidates. The next challenge is to identify other heat-stress-responsive proteins that contribute to the decrease in free Ub chains.

It could be argued that the disappearance of Ub chains upon heat shock is caused by the direct use of Ub chains to a substrate. Recent studies have shown that E2-charged polyubiquitin chains can be directly transferred to a substrate (Li et al., 2007; Ravid and Hochstrasser, 2007). However, this mechanism does not appear to be applied at heat shock because we confirmed that free Ub chains are not E2 charged: yeast lysate treated with dithiothreitol (DTT), a reducing reagent, and DTT-untreated lysate, which should retain the thioester-linkage with E2, showed a similar Ub profile (data not shown).

Increase of Doa4-3×HA and decrease of Rfu1-3×Flag proteins were observed upon heat shock. Heat shock also changes the mRNA levels of *DOA4* and *RFU1* (Gasch et al., 2000). Several genes involved in ribosome transport and assembly show mRNA expression patterns similar to that of *RFU1* upon heat stress (Gasch et al., 2000). Synthesis of many ribosomal proteins is sensitive to high temperature, thus explaining the drop in protein synthesis upon heat shock (Woolford and Warner, 1991). The regulation of Rfu1 expression may be under a similar control. In addition to the regulation of mRNA, we found that heat shock specifically degraded Rfu1-3×Flag protein. Thus, the expression of Rfu1 is regulated by both mRNA and protein levels. We are currently investigating the system involved in Rfu1 protein degradation.

Unanchored Ub Chains as a Reservoir for Monomeric Ub?

If we apply the scenario of disassembling of free Ub chains by DUBs, one can assume that free Ub chains function not only as inhibitors of the 26S proteasome as proposed previously (Amerik et al., 1997) but also as a reservoir for Ubs, which can rapidly provide the cell with monomeric Ubs when more Ub is needed, such as under various stress conditions or stimuli (e.g., heat, chemical treatments, electronic pulses, etc.) (Figure 7). Alternatively, keeping Ubs in the form of free Ub chains may be an efficient way to reduce excess monomeric Ubs, thus preventing unnecessary ubiquitination of cellular proteins.

Consistent with this hypothesis, the double mutants of *Δrfu1* and a component of the UPS (*cdc48-3, ΔN rpn2, rpt1/cim5-1*) contained much more HMW ubiquitinated proteins and were more sensitive to higher temperatures than the single mutant (Figures 1C–1E, 2B, and S4). As more monomeric Ubs are provided by disruption of *RFU1*, overload of the ubiquitination process would occur in the *Δrfu1* mutant and may result in further accumulation of HMW ubiquitinated proteins in the double mutants. Consistently, Ub overproduction was toxic to *cdc48-3* and *cdc48-3Δrfu1* cells (Figure S5). Conversely, overexpression of *RFU1* suppressed the temperature-sensitive growth phenotype of *cdc48-3*, in which Rfu1 was originally isolated in the screening, as well as decreased accumulation of HMW ubiquitinated proteins in *cdc48-3* (Figures 1B and 2C). Thus, consistent with a previous report (London et al., 2004), these ubiquitinated proteins probably cause damage to cells, leading to sensitivity to elevated temperatures. The concept of a free Ub chain acting as a Ub reservoir is reminiscent of glycogen as a storage form of glucose (Stryer, 1981). Excess glucose is stored in the form of glycogen, a chained form of glucose, to maintain glucose concentration in blood at adequate levels. When more glucose is required, glycogen is rapidly hydrolyzed to produce glucose.

As a candidate checkpoint factor for Ub homeostasis, further exploration of the molecular function of Rfu1 will certainly provide a better understanding of Ub homeostasis and of the stress response. Moreover, since free Ub chains exist in various organisms (van Nocker and Vierstra, 1993), it is conceivable that regulation of Ub homeostasis by free Ub chains is a universal mechanism.

EXPERIMENTAL PROCEDURES

Immunoblotting

Preparation of whole-cell extracts and immunoblot analysis were performed essentially as described previously (Kimura et al., 2001), except cells were harvested in the early log phase. To determine the effect of 3×HA-Rfu1 overexpression on Ub profile and stress tolerance, fresh colonies after plasmid transformation were directly suspended in medium and cultured. To analyze the overall Ub profile, total cell proteins were separated by 4%–20% or 10%–20% gradient gels (Bio-Rad, Hercules, CA, USA) using glycine- or tricine-based buffer, followed by transfer to Immobilon-P membranes (Millipore, Bedford, MA, USA). Blots were incubated with mouse anti-Ub monoclonal antibody, MAB1510 (Chemicon International, Inc., Temecula, CA, USA), anti-HA antibody (HA.11, COVANCE, Princeton, NJ, USA), or anti-yeast PGK antibody (Molecular Probes, Eugene, OR, USA), followed by horseradish peroxidase (HRP)-conjugated anti-mouse IgG (#NA931V Amersham Biosciences, Arlington Heights, IL, USA), and detected using ECL-plus reagents (Amersham Biosciences). Rabbit anti-Hsp104 antibody was purchased from Stressgen (Ann Arbor, MI, USA).

Immunoprecipitation

For immunoprecipitation of Rfu1-3×Flag, cells were grown to early logarithmic phase and harvested by centrifugation. Cells were lysed in buffer A (10 mM Tris HCl, pH 7.5, 50 mM potassium acetate, 2 mM EDTA, 10% glycerol, 5 μg/ml pepstatin A, and protease inhibitor cocktail [Roche]) with multi-beads shocker (Yasui Kikai), and Triton X-100 was added at a final concentration of 0.5%. Lysates were centrifuged and the supernatant was incubated with anti-Flag M2 agarose (Sigma) for 2 hr in cold room. After washing with buffer A plus 0.5% Triton X-100, the immunocomplex was eluted by 1× sample buffer and analyzed by western blotting. The blots were incubated with anti-HA, anti-myc (9E10, Santa Cruz Biotechnology), or anti-Flag antibody (Sigma).

For immunoprecipitation of GFP-CPS, cells were lysed in buffer A with a multi-beads shocker. After centrifugation, the supernatants were incubated with anti-GFP antibody (Roche) and Protein G sepharose. The immunocomplex was washed with buffer A plus 1% Triton X-100 and 200 mM NaCl, eluted with 1× sample buffer, and analyzed by western blotting.

In Vitro Binding of MBP-Rfu1 with FVH-Doa4

Maltose-binding protein (MBP) or MBP-Rfu1 (each 5 μg) was mixed with FVH-Doa4 or FVH-Yuh1 (each 4 μg) in buffer B (50 mM Tris-HCl, pH 7.5, 100 mM NaCl, 10% glycerol, and 0.5% Triton X-100) for 1 hr at 25°C followed by the addition of amylose resin. After 30 min, the resin was washed with buffer B and eluted with buffer B containing 10 mM maltose. The eluted samples were analyzed by western blotting.

In Vitro Doa4 Deubiquitinating Assay

The DUB activity of FVH-Doa4 and its mutant was tested with K48-linked and K63-linked polyubiquitin (Biomol International, 1 μg each per reaction) in 100 mM Tris-HCl, pH 7.5, 100 mM KCl, 100 mM $MgCl_2$, 100 mM DTT, and 1.9% glycerol. To determine the effect of MBP-Rfu1 or MBP, the proteins were mixed with FVH-Doa4 for 15 min prior to the addition of polyubiquitin. Reactions were incubated for 2 or 3 hr at 25°C, mixed with a sample buffer, and heated at 37°C for 30 min. They were analyzed by immunoblotting using anti-Ub antibody (P4D1).

SUPPLEMENTAL DATA

Supplemental Data include Supplemental Experimental Procedures, 11 figures, 2 tables, and Supplemental References and can be found with this article online at http://www.cell.com/supplemental/S0092-8674(09)00204-9.

ACKNOWLEDGMENTS

We thank T. Fujita for his initial support and C. Takahashi, H. Ueno, and T. Hasegawa for technical support. We also thank D. Botstein, K. Matsumoto, K. Umebayashi, R. Hirata, A. Nakano, Y. Saeki, S. Ito, and A. Amerik for materials, Y. Saeki, K. Umebayashi, R. Hirata, A. Nakano, A. Toh-e, Y. Yoshida, and N. Matsuda for discussion, and A. Toh-e for comments on the manuscript. This work was supported by Grants-in-Aid for Scientific Research on Priority Area (to Y.K.), Specially Promoted Research (to K.T.) from the Ministry of Education, Culture, Science and Technology of Japan, the Target Protein Project of MEXT (to K.T.), and Takeda Science Foundation (to K.T.).

Received: November 30, 2007
Revised: November 14, 2008
Accepted: February 6, 2009
Published: April 30, 2009

REFERENCES

Amerik, A.Y., and Hochstrasser, M. (2004). Mechanism and function of deubiquitinating enzymes. Biochim. Biophys. Acta *1695*, 189–207.

Amerik, A., Swaminathan, S., Krantz, B.A., Wilkinson, K.D., and Hochstrasser, M. (1997). In vivo disassembly of free polyubiquitin chains by yeast Ubp14 modulates rates of protein degradation by the proteasome. EMBO J. *16*, 4826–4838.

Amerik, A.Y., Li, S.J., and Hochstrasser, M. (2000a). Analysis of the deubiquitinating enzymes of the yeast *Saccharomyces cerevisiae*. Biol. Chem. *381*, 981–992.

Amerik, A.Y., Nowak, J., Swaminathan, S., and Hochstrasser, M. (2000b). The Doa4 deubiquitinating enzyme is functionally linked to the vacuolar protein-sorting and endocytic pathways. Mol. Biol. Cell *11*, 3365–3380.

Amerik, A., Sindhi, N., and Hochstrasser, M. (2006). A conserved late endosome-targeting signal required for Doa4 deubiquitylating enzyme function. J. Cell Biol. *175*, 825–835.

Carlson, N., Rogers, S., and Rechsteiner, M. (1987). Microinjection of ubiquitin: changes in protein degradation in HeLa cells subjected to heat-shock. J. Cell Biol. *104*, 547–555.

Chen, Y., and Piper, P.W. (1995). Consequences of the overexpression of ubiquitin in yeast: elevated tolerances of osmostress, ethanol and canavanine, yet reduced tolerances of cadmium, arsenite and paromomycin. Biochim. Biophys. Acta *1268*, 59–64.

Chernova, T.A., Allen, K.D., Wesoloski, L.M., Shanks, J.R., Chernoff, Y.O., and Wilkinson, K.D. (2003). Pleiotropic effects of Ubp6 loss on drug sensitivities and yeast prion are due to depletion of the free ubiquitin pool. J. Biol. Chem. *278*, 52102–52115.

Dupre, S., and Haguenauer-Tsapis, R. (2001). Deubiquitination step in the endocytic pathway of yeast plasma membrane proteins: crucial role of Doa4p ubiquitin isopeptidase. Mol. Cell. Biol. *21*, 4482–4494.

Finley, D., Ozkaynak, E., and Varshavsky, A. (1987). The yeast polyubiquitin gene is essential for resistance to high temperatures, starvation, and other stresses. Cell *48*, 1035–1046.

Fiorani, P., Reid, R.J., Schepis, A., Jacquiau, H.R., Guo, H., Thimmaiah, P., Benedetti, P., and Bjornsti, M.A. (2004). The deubiquitinating enzyme Doa4p protects cells from DNA topoisomerase I poisons. J. Biol. Chem. *279*, 21271–21281.

Gasch, A.P., Spellman, P.T., Kao, C.M., Carmel-Harel, O., Eisen, M.B., Storz, G., Botstein, D., and Brown, P.O. (2000). Genomic expression programs in the response of yeast cells to environmental changes. Mol. Biol. Cell *11*, 4241–4257.

Ghaemmaghami, S., Huh, W.K., Bower, K., Howson, R.W., Belle, A., Dephoure, N., O'Shea, E.K., and Weissman, J.S. (2003). Global analysis of protein expression in yeast. Nature *425*, 737–741.

Ghislain, M., Udvardy, A., and Mann, C. (1993). S. cerevisiae 26S protease mutants arrest cell division in G2/metaphase. Nature *366*, 358–362.

Ghislain, M., Dohmen, R.J., Levy, F., and Varshavsky, A. (1996). Cdc48p interacts with Ufd3p, a WD repeat protein required for ubiquitin-mediated proteolysis in Saccharomyces cerevisiae. EMBO J. *15*, 4884–4899.

Hanna, J., Meides, A., Zhang, D.P., and Finley, D. (2007). A ubiquitin stress response induces altered proteasome composition. Cell *129*, 747–759.

Hershko, A., and Ciechanover, A. (1998). The ubiquitin system. Annu. Rev. Biochem. *67*, 425–479.

Hodgins, R.R., Ellison, K.S., and Ellison, M.J. (1992). Expression of a ubiquitin derivative that conjugates to protein irreversibly produces phenotypes consistent with a ubiquitin deficiency. J. Biol. Chem. *267*, 8807–8812.

Huh, W.K., Falvo, J.V., Gerke, L.C., Carroll, A.S., Howson, R.W., Weissman, J.S., and O'Shea, E.K. (2003). Global analysis of protein localization in budding yeast. Nature *425*, 686–691.

Isono, E., Nishihara, K., Saeki, Y., Yashiroda, H., Kamata, N., Ge, L., Ueda, T., Kikuchi, Y., Tanaka, K., Nakano, A., and Toh-e, A. (2007). The assembly pathway of the 19S regulatory particle of the yeast 26S proteasome. Mol. Biol. Cell *18*, 569–580.

Johnson, E.S., Ma, P.C.M., Ota, I.M., and Varshavsky, A. (1995). A proteolytic pathway that recognizes ubiquitin as a degradation signal. J. Biol. Chem. *270*, 17422–17456.

Katzmann, D.J., Babst, M., and Emr, S.D. (2001). Ubiquitin-dependent sorting into the multivesicular body pathway requires the function of a conserved endosomal protein sorting complex, ESCRT-I. Cell *106*, 145–155.

Kimura, Y., Koitabashi, S., Kakizuka, A., and Fujita, T. (2001). Initial process of polyglutamine aggregate formation in vivo. Genes Cells *6*, 887–897.

Li, W., Tu, D., Brunger, A.T., and Ye, Y. (2007). A ubiquitin ligase transfers preformed polyubiquitin chains from a conjugating enzyme to a substrate. Nature *446*, 333–337.

London, M.K., Keck, B.I., Ramos, P.C., and Dohmen, R.J. (2004). Regulatory mechanisms controlling biogenesis of ubiquitin and proteasome. FEBS Lett. *567*, 259–264.

Luhtala, N., and Odorizzi, G. (2004). Bro1 coordinates deubiquitination in the multivesicular body pathway by recruiting Doa4 to endosomes. J. Cell Biol. *166*, 717–729.

McCullough, J., Clague, M.J., and Urbe, S. (2004). AMSH is an endosome-associated ubiquitin isopeptidase. J. Cell Biol. *166*, 487–492.

Mukhopadhyay, D., and Riezman, H. (2007). Proteasome-independent functions of ubiquitin in endocytosis and signaling. Science *315*, 201–205.

Naviglio, S., Mattecucci, C., Matoskova, B., Nagase, T., Nomura, N., Di Fiore, P.P., and Draetta, G.F. (1998). UBPY: a growth-regulated human ubiquitin isopeptidase. EMBO J. *17*, 3241–3250.

Nikko, E., and Andre, B. (2007). Evidence for a direct role of the Doa4 deubiquitinating enzyme in protein sorting into the MVB pathway. Traffic *8*, 566–581.

Osaka, H., Wang, Y.L., Takada, K., Takizawa, S., Setsuie, R., Li, H., Sato, Y., Nishikawa, K., Sun, Y.J., Sakurai, M., et al. (2003). Ubiquitin carboxy-terminal hydrolase L1 binds to and stabilizes monoubiquitin in neuron. Hum. Mol. Genet. *12*, 1945–1958.

Papa, F.R., and Hochstrasser, M. (1993). The yeast DOA4 gene encodes a deubiquitinating enzyme related to a product of the human tre-2 oncogene. Nature *366*, 313–319.

Papa, F.R., Amerik, A.Y., and Hochstrasser, M. (1999). Interaction of the Doa4 deubiquitinating enzyme with the yeast 26S proteasome. Mol. Biol. Cell *10*, 741–756.

Pickart, C.M., and Eddins, M.J. (2004). Ubiquitin: structures, functions, mechanisms. Biochim. Biophys. Acta *1695*, 55–72.

Ravid, T., and Hochstrasser, M. (2007). Autoregulation of an E2 enzyme by ubiquitin-chain assembly on its catalytic residue. Nat. Cell Biol. *9*, 422–427.

Richter, C., West, M., and Odorizzi, G. (2007). Dual mechanisms specify Doa4-mediated deubiquitination at multivesicular bodies. EMBO J. *26*, 2454–2464.

Row, P.E., Liu, H., Hayes, S., Welchman, R., Charalabous, P., Hofmann, K., Clague, M.J., Sanderson, C.M., and Urbe, S. (2007). The MIT domain of UBPY constitutes a CHMP binding and endosomal localization signal required for efficient epidermal growth factor receptor degradation. J. Biol. Chem. *282*, 30929–30937.

Ryu, K.Y., Maehr, R., Gilchrist, C.A., Long, M.A., Bouley, D.M., Mueller, B., Ploegh, H.L., and Kopito, R.R. (2007). The mouse polyubiquitin gene UbC is essential for fetal liver development, cell-cycle progression and stress tolerance. EMBO J. *26*, 2693–2706.

Ryu, K.Y., Garza, J.C., Lu, X.Y., Barsh, G.S., and Kopito, R.R. (2008). Hypothalamic neurodegeneration and adult-onset obesity in mice lacking the Ubb polyubiquitin gene. Proc. Natl. Acad. Sci. USA *105*, 4016–4021.

Schnell, J.D., and Hicke, L. (2003). Non-traditional functions of ubiquitin and ubiquitin-binding proteins. J. Biol. Chem. *278*, 35857–35860.

Singer, J.D., Manning, B.M., and Formosa, T. (1996). Coordinating DNA replication to produce one copy of the genome requires genes that act in ubiquitin metabolism. Mol. Cell. Biol. *16*, 1356–1366.

Stryer, L. (1981). Biochemistry, Second Edition (New York: W.H. Freeman and Company).

Swaminathan, S., Amerik, A.Y., and Hochstrasser, M. (1999). The Doa4 deubiquitinating enzyme is required for ubiquitin homeostasis in yeast. Mol. Biol. Cell *10*, 2583–2594.

van Nocker, S., and Vierstra, R.D. (1993). Multiubiquitin chains linked through lysine 48 are abundant in vivo and are competent intermediates in the ubiquitin proteolytic pathway. J. Biol. Chem. *268*, 24766–24773.

Ventii, K.H., and Wilkinson, K.D. (2008). Protein partners of deubiquitinating enzymes. Biochem. J. *414*, 161–175.

Woodman, P.G. (2003). p97, a protein coping with multiple identities. J. Cell Sci. *116*, 4283–4290.

Woolford, J.J., and Warner, J.R. (1991). The ribosome and its synthesis. In The Molecular and Cellular Biology of the Yeast Saccharomyces, J.R. Broach, J.R. Pringle, and E.W. Jones, eds. (Cold Spring Harbor, NY: Cold Spring Harbor Laboratory Press), pp. 587–626.

Xu, P., and Peng, J. (2008). Characterization of polyubiquitin chain structure by middle-down mass spectrometry. Anal. Chem. *80*, 3438–3444.

Cell

Multiple Proteasome-Interacting Proteins Assist the Assembly of the Yeast 19S Regulatory Particle

Yasushi Saeki,[1] Akio Toh-e,[1,*] Tai Kudo,[1] Hitomi Kawamura,[1] and Keiji Tanaka[1,*]
[1]Laboratory of Frontier Science, Core Technology and Research Center, Tokyo Metropolitan Institute of Medical Science, 2-1-6 Kamikitazawa, Setagaya-ku, Tokyo 156-8506, Japan
*Correspondence: toue-ak@igakuken.or.jp (A.T.), tanaka-kj@igakuken.or.jp (K.T.)
DOI 10.1016/j.cell.2009.05.005

SUMMARY

The 26S proteasome is a highly conserved multisubunit protease that degrades ubiquitinated proteins in eukaryotic cells. The 26S proteasome consists of the proteolytic core particle (CP) and one or two 19S regulatory particles (RPs). Although the mechanisms of CP assembly are well described, the mechanism of RP assembly is largely unknown. Here, we show that four proteasome-interacting proteins (PIPs), Nas2/p27, Nas6/gankyrin, Rpn14/PAAF1, and Hsm3/S5b, bind specific Rpt subunits of the RP and interact each other genetically. Lack of these PIPs resulted in defective assembly of the 26S proteasome at an early stage, suggesting that these proteins are bona fide RP chaperones. Each of the RP chaperones formed distinct specific subassemblies of the base components and escorted them to mature RPs. Our results indicate that the RP assembly is a highly organized and elaborate process orchestrated by multiple proteasome-dedicated chaperones.

INTRODUCTION

The eukaryotic 26S proteasome is a multicatalytic enzyme responsible for degradation of a large fraction of intracellular proteins (Baumeister et al., 1998; Coux et al., 1996; Hershko and Ciechanover, 1998). Most proteins destined for degradation by the proteasome are marked with polyubiquitin chains, which serve as a target signal for the 26S proteasome. The ubiquitin-proteasome system (UPS) controls a diverse array of biologically important processes, including cell-cycle progression, DNA repair, signal transduction, and protein quality control. The 26S proteasome acts at the final step of this pathway by degrading polyubiquitinated protein substrates, ensuring the irreversibility of the aforementioned biological processes. Defects in this system result in the pathogenesis of several severe human diseases (Schwartz and Ciechanover, 2009).

The 26S proteasome is composed of at least 33 different subunits arranged in two complexes, the 20S core particle (CP; also known as 20S proteasome) and one or two 19S regulatory particles (RPs). The RP binds to one or both ends of the latent CP to form an enzymatically active 26S proteasome, referred to as RP_1CP and RP_2CP, respectively. The proteolytic sites are sequestered inside the CP and are accessible only through a narrow channel so that substrate proteins must be unfolded to reach the proteolytic sites. The RP recognizes the polyubiquitin chains, deconjugates ubiquitin chains, unfolds substrate proteins, and translocates them into the catalytic CP. The CP is composed of two outer rings, each consisting of seven α subunits, and two inner rings, each consisting seven β subunits. Three of the seven β subunits have proteolytic sites that face the inner chamber of the CP. On the other hand, the 19S RP contains approximately 19 different subunits that can be subclassified into two groups—regulatory particle ATPase (Rpt) subunits and regulatory particle non-ATPase (Rpn) subunits—both of which contain multiple proteins with molecular masses ranging from 10 to 110 kDa. The RP is composed of two major subcomplexes, the base and lid (Glickman et al., 1998). The base consists of six ATPase subunits (Rpt1–6) and three non-ATPase subunits (Rpn1, 2, 13), while the lid is made up of nine non-ATPase subunits (Rpn3, 5–9, 12, and Sem1/Rpn15) (Leggett et al., 2005; Murata et al., 2009). The base-lid association is stabilized by another subunit, Rpn10 (Glickman et al., 1998). In addition, numerous proteasome-interacting proteins (PIPs) that regulate the activities of the proteasome have been identified, including extrinsic ubiquitin receptors Rad23 and Dsk2, deubiquitinating enzyme Ubp6, and ubiquitin ligase Hul5 in yeast (Hanna and Finley, 2007; Leggett et al., 2002; Verma et al., 2000).

How the proteasome subunits organize themselves into such a huge and complex structure is a fundamental question for our understanding of intracellular proteolysis and dynamic changes in the proteasome. The discovery of the 20S proteasome-specific chaperones, Ump1 and PAC1-4, revealed that CP biogenesis is a highly ordered multistep event rather than a simple self-assembly (Kusmierczyk et al., 2008; Murata et al., 2009; Ramos and Dohmen, 2008). In contrast, the process involved in the assembly of the RP from its individual components is largely unknown, although there is evidence that the lid and base can be assembled independently of each other (Isono et al., 2007). Nob1, an Rpn12-interacting protein, is considered an assembly factor for the 26S proteasome (Tone and Toh-e, 2002), but its significance in this role has been challenged (Fatica et al., 2003). Genetic data have indicated that the

Hsp90 chaperone plays a role in the assembly and maintenance of the 26S proteasome (Imai et al., 2003). In *Schizosaccaromyces pombe*, Yin6, an ortholog of mammalian INT6, has been proposed to incorporate Rpn5 into the 26S proteasome (Yen and Chang, 2003), but INT6 also seems to regulate the lid-related complexes COP9/signalosome and eIF3 (Rencus-Lazar et al., 2008; Yahalom et al., 2008). Despite extensive genetic and biochemical studies, the molecular mechanisms underlying the RP assembly are mostly unknown.

We isolated previously the human p28 and its yeast ortholog Nas6 as a putative subunit of the 26S proteasome (Hori et al., 1998). p28 is also known as gankyrin that is overexpressed in hepatocellular carcinomas (Dawson et al., 2002; Higashitsuji et al., 2000). In our search for functions of Nas6, we found that it interacted genetically with multiple PIPs: Nas2, Rpn14, and Hsm3. In the absence of these PIPs, most 26S proteasomes disappeared because of the assembly defect of the base subcomplex, suggesting that these PIPs function as bona fide RP chaperones. Each of the RP chaperones forms a distinct subassembly of the base components and escorts them to mature RPs. These results suggest that the chaperone-assisted RP assembly is a highly ordered and elaborate process in eukaryotic cells.

RESULTS

Nas6, the Yeast Ortholog of Gankyrin, Affects Proteasome Activity

Human gankyrin (alias p28) has been proposed to function as a bridging factor between the proteasome and various substrates such as pRb and p53 (reviewed in Lozano and Zambetti, 2005). Although the yeast ortholog Nas6 shares high sequence homology with human gankyrin (Dawson et al., 2002; Hori et al., 1998; Nakamura et al., 2007b), the precise role of Nas6 in yeast cells is poorly understood. To investigate the function of Nas6, we performed several genetic studies and found that overproduction of *NAS6* was toxic specifically in the *Δrpn9* lid mutant cell (Figure 1A), which exhibits destabilization of the 26S proteasome and accumulation of polyubiquitinated proteins (Takeuchi et al., 1999). Although the *NAS6* deleted strain grew normally (Dawson et al., 2002; Hori et al., 1998), we noticed that the *Δnas6* cell shows mild sensitivity to the proline analog, L-azetidine-2-carboxylic acid (AZC), as observed in other proteasome mutants, *Δrpn10* and *Δpre9* cells (Figure 1B). These genetic results suggest the involvement of Nas6 in the UPS, similar to gankyrin in mammalian cells.

Rpn14 Is Functionally Related to Nas6

Because the *Δnas6* single mutant cells showed only a mild defect as described above, we hypothesized that other genes buffer the single deletion. To test this, we crossed the *Δnas6* strain with a series of mutants that include the ~40 known UPS-related genes. Within the generated double mutants, the *Δnas6 Δrpn14* double-deletion strain showed a severe growth defect at 37°C (Figure 1C). In yeast, Rpn14 is a putative RP subunit required for the degradation of certain proteasome substrates (Samanta and Liang, 2003; Seong et al., 2007). In contrast, its mammalian ortholog, named proteasomal ATPase-associated factor 1 (PAAF1), is a negative regulator of the 26S proteasome and facilitates transcription in mammalian cells (Lassot et al., 2007).

We first analyzed the accumulation of polyubiquitinated proteins in the *Δnas6 Δrpn14* double-deletion strain. Under restrictive temperatures, the polyubiquitinated proteins accumulated in the *Δnas6 Δrpn14* cells but not in the respective single mutants (Figure 1D). This result suggests that the functions of Nas6 and Rpn14 are redundant and that both Nas6 and Rpn14 positively regulate the degradation of ubiquitinated proteins.

Next, we analyzed the interaction between Nas6, Rpn14, and proteasomal complexes using three tandem FLAG epitope-tagged strains: C-terminal-tagged *NAS6*, N-terminal-tagged *RPN14*, and a control strain 3xFLAG-tagged *RPN11*. Cell extracts were prepared in the presence of ATP and then fractionated by native-polyacrylamide gel electrophoresis (PAGE), followed by western blotting with anti-Flag antibody (Figure 1E). As reported previously in mammalian cells (Dawson et al., 2002), Nas6 was detected in both free and complex forms. Interestingly, Rpn14 was also detected in free and complex forms, similar to Nas6 (Figure 1E). Both the Nas6- and Rpn14-containing complexes were smaller than the 26S proteasomes (RP_1CP and RP_2CP) and were identified as the RP and base complexes, respectively (data not shown; see below also). Immunoprecipitates from either the *NAS6-3xFLAG* or *3xFLAG-RPN14* strain contained the RP subunits but lacked the CP subunits (Figures 1F and 1G).

In the Rpn14-containing complex, a relatively highly abundant protein was detected and identified as Nas6 by mass spectrometry (MS), suggesting that the Rpn14-containing complex also contains Nas6 (Figure 1G). To further characterize the Nas6- and Rpn14-containing complexes, the immunoprecipitates were digested with trypsin and subjected to nano liquid chromatography (LC)-coupled MS. From the immunoprecipitates of both, we identified all of the RP subunits, especially the base subunits, with high scores (Figure 1H), indicating that both Nas6 and Rpn14 associate mainly with the base subcomplex consistent with the above result (Figure 1E). In addition to the RP subunits, other PIPs, Nas2 and Hsm3, were unexpectedly identified from the immunoprecipitates (Figure 1H). Extracts of *NAS2-3xFLAG* and *HSM3-3xFLAG* cells were also analyzed by native-PAGE. Similar to Nas6 and Rpn14, Nas2 and Hsm3 were detected in both free and complex forms but not in 26S proteasomes (data not shown).

Four Distinct PIPs—Nas6, Nas2, Rpn14, and Hsm3—Bind Specific Rpt Subunits and Localize in Both the Cytosol and Nucleus

Nas2 is an ortholog of the p27 subunit of the mammalian proteasome modulator, which consists of p27, Rpt4, and Rpt5 (DeMartino et al., 1996), whereas Hsm3 is a putative ortholog of the mammalian RP subunit S5b, which can form a complex with Rpn1, Rpt1, and Rpt2 in vitro (Deveraux et al., 1995). Although both *NAS2* and *HSM3* are not essential (Russell et al., 1999; Watanabe et al., 1998), the latter is involved in correct DNA replication (Fedorova et al., 1998, 2004).

Although there are no obvious sequence similarities among Nas2, Nas6, Rpn14, and Hsm3, each PIP has a distinct characteristic module for protein-protein interactions. For example, Nas2 contains a PDZ domain, Nas6 contains ankyrin repeats, Rpn14 contains WD40 repeats, and Hsm3 contains HEAT

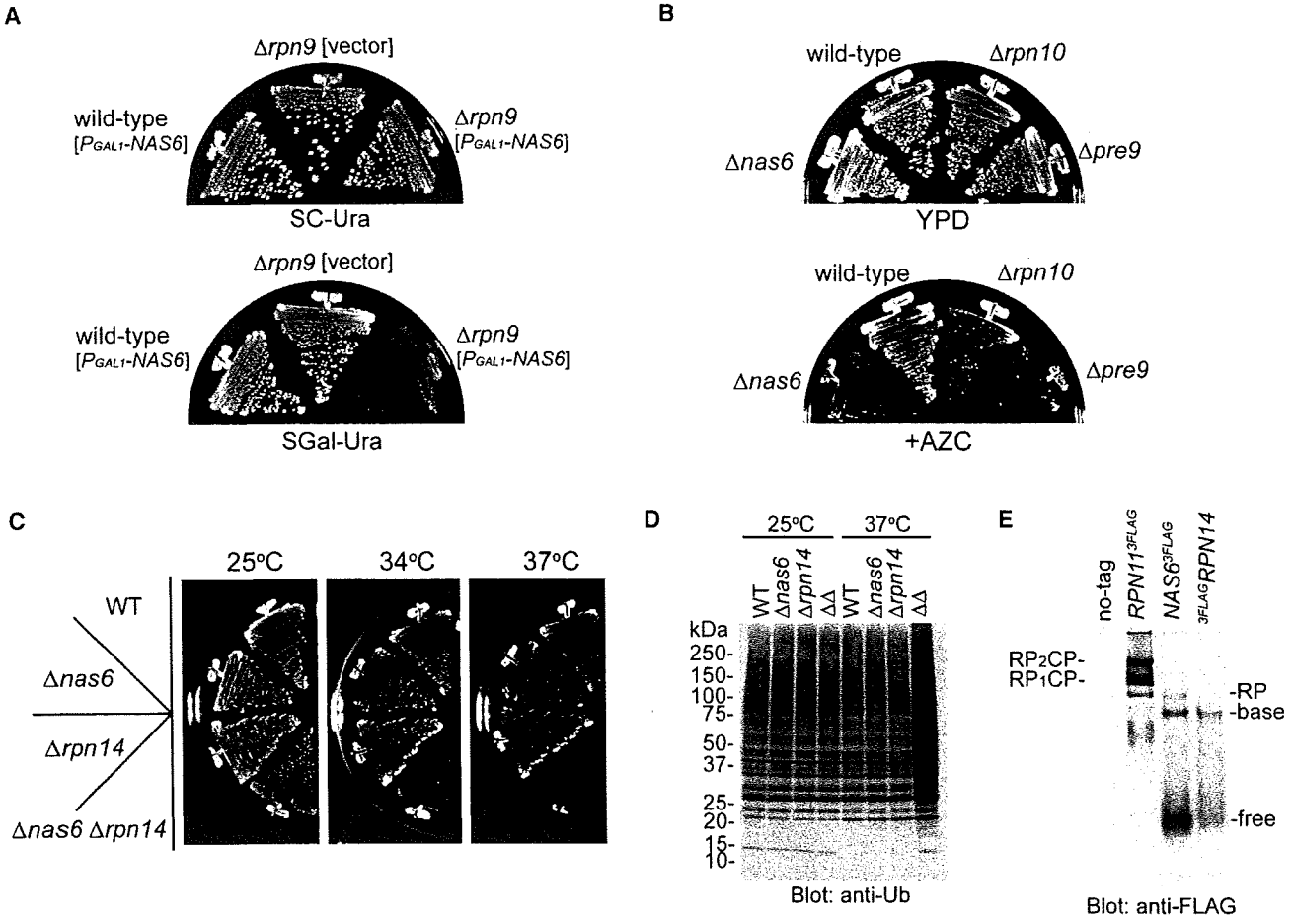

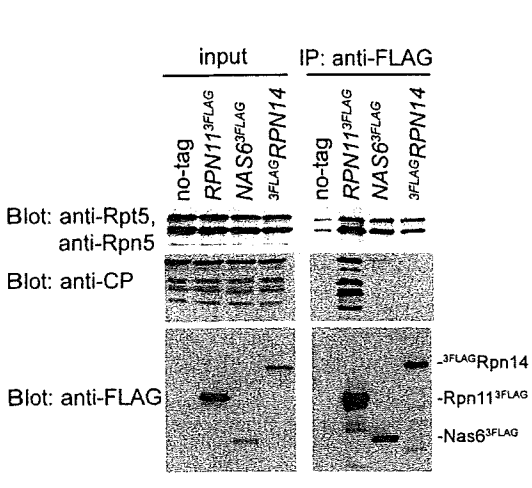

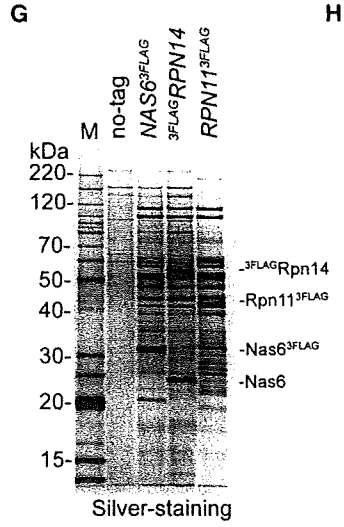

H

NAS6 3FLAG	*3FLAG RPN14*
Rpn2 (56.2%)	Rpn2 (53.7%)
Rpt1 (76.4%)	**Rpn14 (73.1%)**
Rpt3 (91.6%)	Rpt5 (75.8%)
Rpt5 (75.6%)	Rpt1 (72.8%)
Rpt6 (89.6%)	Rpt6 (87.9%)
Rpt2 (72.5%)	Rpt3 (80.1%)
Rpn1 (37.1%)	Rpt4 (77.6%)
Rpt4 (78.9%)	Rpn1 (42.1%)
Rpn14 (56.1%)	Rpt2 (77.6%)
Nas6 (75.0%)	Rpn3 (32.6%)
Rpn8 (77.5%)	Rpn11 (52.6%)
Rpn11 (79.1%)	**Nas6(50.4%)**
Ubp6 (57.3%)	**Nas2(64.1%)**
Rpn3 (40.4%)	Rpn10 (59.0%)
Rpn6 (45.9%)	Rpn8 (64.8%)
Rpn5 (37.8%)	Rpn13 (58.3%)
Rpn13 (69.9%)	Rpn5 (35.1%)
Rpn10 (52.2%)	Rpn6 (50.7%)
Rpn7 (45.2%)	**Hsm3(28.8%)**
Rpn9 (49.4%)	Rpn7 (29.4%)
Rpn12 (23.7%)	Rpn9 (27.2%)
Hsm3 (26.7%)	Rpn12 (31.8%)
Nas2 (37.3%)	Ubp6 (20.6%)
Sem1 (25.8%)	

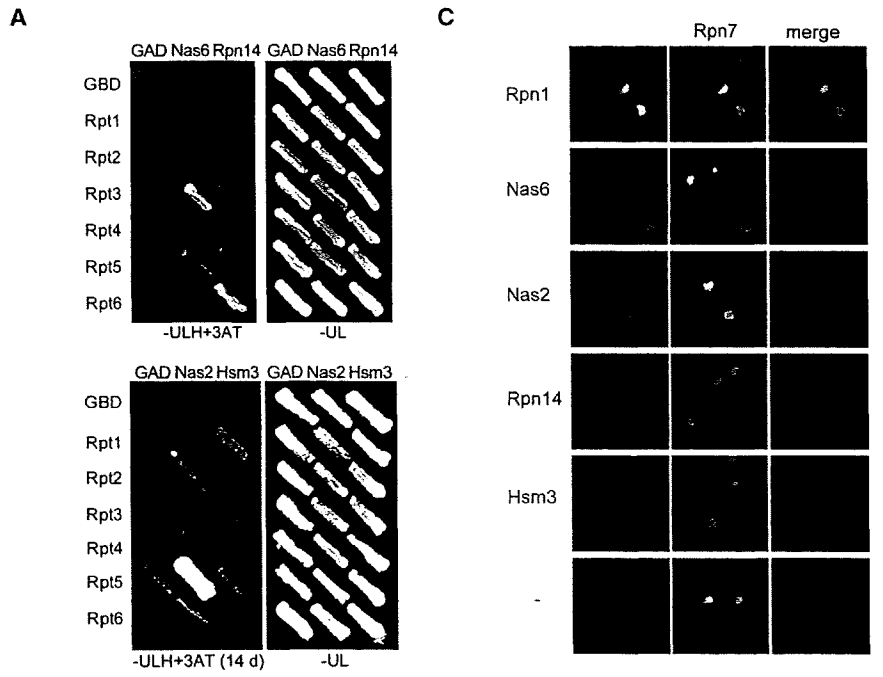

Figure 2. Nas6, Nas2, Rpn14, and Hsm3 Have Similar Properties

(A) Nas6, Nas2, Rpn14, and Hsm3 each bind a specific Rpt subunit. Yeast cells (PJ69-4A) transformed with the indicated combinations of bait (pGBD) and prey (pGAD) plasmids were assayed with *HIS3*-based selection. The cells were streaked onto SC plates lacking uracil and leucine (-UL) or lacking uracil, leucine, histidine, and 3 amino-triazole (-ULH+3AT) and incubated for 5–14 days.

(B) Nas6, Nas2, Rpn14, and Hsm3 each specifically bind to the C-terminal region of the respective Rpt subunits. Various constructs of Rpt subunits, depicted in light, were fused to a bait plasmid and tested as in (A). SC plates lacking uracil, leucine, histidine, and adenine (-ULHA) were also used for more stringent condition than SC-ULH.

(C) Nas6, Nas2, Rpn14, and Hsm3 each localize mainly in the cytosol. Wild-type cells expressing Rpn7-mCherry and either yEGFP1F-tagged Rpn1, Nas2, Nas6, Rpn14, or Hsm3 (YYS1601, Hiy128-131) were imaged by a confocal microscope. Cells expressing Rpn7-mCherry (YYS1392) only were also used as control.

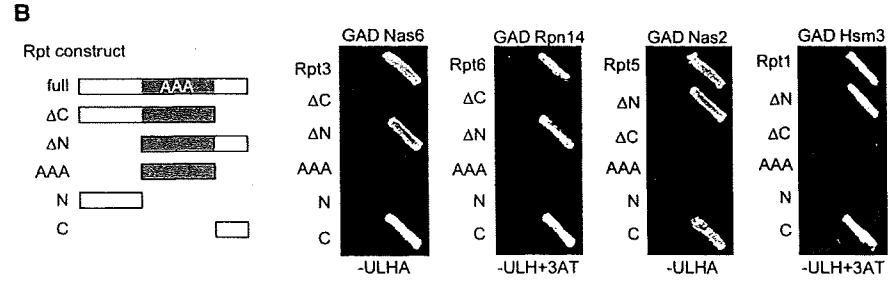

repeats. The fact that all of these PIPs can bind simultaneously to the base subcomplex (Figure 1) suggests that these PIPs bind different specific base subunits. To test this, we investigated the interactions between these PIPs and all nine base subunits by using the yeast two-hybrid (Y2H) assay. As reported previously (Nakamura et al., 2007b), Nas6 specifically bound Rpt3 (Figure 2A). Furthermore, specific PIP-Rpt pairs were detected: Rpn14-Rpt6, Nas2-Rpt5, and Hsm3-Rpt1 (Figure 2A). We failed to detect the binding of the other base subunits, Rpn1, Rpn2, and Rpn13, with the four PIPs by Y2H (data not shown). Moreover, these PIPs did not bind with the purified lid complex in vitro (data not shown). The eukaryotic proteasome contains six essential ATPase subunits (i.e., Rpt1–6), which contain a conserved ATPase domain and variable N-terminal and C-terminal domains (Pickart and Cohen, 2004). Crystallographic studies have shown that the C-terminal domain of Rpt3 is responsible for Nas6 binding

Figure 1. Genetic and Biochemical Analyses of Nas6 and Rpn14

(A) Overproduction of Nas6 is toxic in the proteasome mutant *Δrpn9* cells. *Δrpn9* (YYS290) and its wild-type strains carrying a high-copy plasmid for galactose-inducible Nas6 expression (P_{GAL1}-*NAS6*) or control vector (vector) were grown on SC-Ura or SGal-Ura plates at 25°C for 2–4 days.

(B) The *Δnas6* cells are sensitive to amino acid analog. Wild-type (WT), *Δnas6* (YYS381), *Δrpn10* (YYS530), and *Δpre9* (#4765) cells were grown on YPD or YPD containing the amino acid analog AZC at 25°C for 2–3 days.

(C) *NAS6* genetically interacts with *RPN14*. Wild-type (WT), *Δnas6* (YYS381), *Δrpn14* (YYS382), and *Δnas6 Δrpn14* (YYS383) cells were grown on YPD plates at the indicated temperatures for 2–3 days.

(D) Accumulation of ubiquitinated proteins in *Δnas6 Δrpn14* cells under restrictive temperature. Cells cultured for 6 hr at 37°C were analyzed by western blotting with anti-ubiquitin antibody.

(E) Both Nas6 and Rpn14 are not detected in 26S proteasomes. Crude lysate from *RPN11-3xFLAG* (YYS40), *NAS6-3xFLAG* (YYS402), and *3xFLAG-RPN14* (YYS528) strains were resolved with 4% native-PAGE followed by western blotting with anti-Flag antibody. Two isoforms of 26S proteasomes are indicated as RP_2CP and RP_1CP.

(F) Nas6 and Rpn14 do not form complexes with the CP. Immunoprecipitates from the respective FLAG-tagged cells were analyzed by western blotting with anti-Rpn5 (lid), anti-Rpt5 (base), anti-CP, and anti-Flag antibodies.

(G) SDS-PAGE analysis of the Nas6- or Rpn14-containing complex. Affinity-purified proteins from the respective Flag-tagged strains were subjected to SDS-PAGE followed by silver staining.

(H) Two additional proteins were identified in the Nas6- and Rpn14-containing complexes. Affinity-purified proteins in (G) were digested with trypsin and subjected to LC-coupled mass spectrometry (MS). Identified proteins with high confidence (>99.9%) are listed in descending order. The sequence coverages of the identified proteins are indicated in parenthesis. Proteins that are not integral RP subunits are highlighted in bold text.

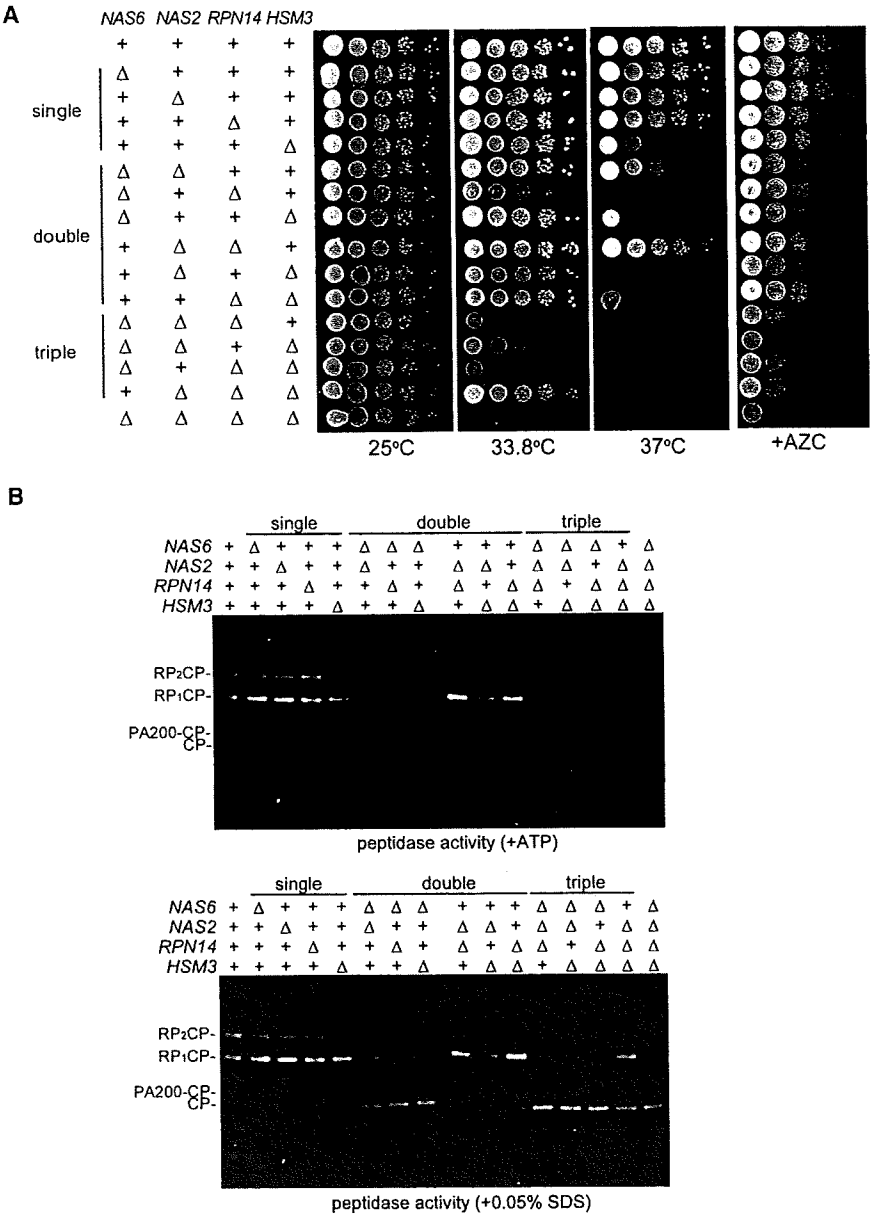

Figure 3. Loss of Nas6, Nas2, Rpn14, and Hsm3 Results in Disassembly of the 26S Proteasome

(A) Multiple deletions of *NAS2*, *NAS6*, *RPN14*, and *HSM3* exhibit temperature- and amino acid-analog sensitivities. Ten-fold serial dilutions of cells (W303a and YYS1201-1215) were spotted onto YPD plates and incubated at 25°C, 33.8°C, or 37°C. YPD plate supplemented with 5 mM AZC was also tested.

(B) Multiple deletions of *NAS2*, *NAS6*, *RPN14*, and *HSM3* result in disassembly of 26S proteasomes. The indicated cells (W303a and YYS1201-1215) were cultured for 4 hr at 37°C. Extracts prepared in the presence of ATP were resolved on 3.5% native-PAGE. The gel was incubated with Suc-LLVY-AMC in the presence of ATP to monitor 26S proteasomes and then in the presence of 0.05% SDS to visualize CP activity. The two isoforms of the 26S proteasome (RP_2CP and RP_1CP), PA200-CP complex, and free CP are indicated.

(Nakamura et al., 2007a, 2007b). To test whether the C-terminal domains of Rpt subunits are also utilized for other PIPs-Rpt interactions, we performed domain analysis by Y2H analysis. Interestingly, the C-terminal domains were found to be required and sufficient for all PIPs bindings (Figure 2B). Recent reports indicated that the C-terminal tails of ATPase subunits are responsible for CP activation by inserting themselves into intersubunit pockets of the CP (Gillette et al., 2008; Rabl et al., 2008; Smith et al., 2007). Hence, the C termini binding proteins, Nas6, Nas2, Rpn14, and Hsm3, locate and occupy the CP binding surface of the RP. This notion is consistent with the above result; i.e., these PIPs exist only in the base or RP but not in the 26S proteasome (Figure 1D).

Next, we investigated the cellular distributions of Nas6, Nas2, Rpn14, and Hsm3 because it has been proposed that there is a tight link between nucleocytoplasmic trafficking and the proteasome subcomplex assembly; each subcomplex of the 26S proteasome (i.e., the CP, base, and lid) can be imported into the nucleus after its formation (Isono et al., 2007). Each of the PIPs was tagged chromosomally with yEGFP1F tag that consists of yeast enhanced green fluorescent protein (yEGFP) and 3xFLAG tag. Note that all of the tagged strains were functional because the tagged genes can suppress the phenotype of their null mutants (Figure S1 available online). As a control, the lid subunit Rpn7 was tagged with monomeric red fluorescent protein (mCherry). In the Rpn1-yEGFP1F Rpn7-mCherry expressing cells, both proteins were colocalized mainly in the nucleus (Figure 2C), in agreement with the previous study that the mature yeast 26S proteasome exists predominantly in the nucleus (Enenkel et al., 1998; Isono et al., 2007; Wendler et al., 2004). In contrast, Nas6-yEGFP1F, Nas2-yEGFP1F, yEGFP1F-Rpn14, and Hsm3-yEGFP1F were observed in both the cytosol and nucleus at lower intensities than that of Rpn1-yEGFP1F (Figure 2C), suggesting that these PIPs function in the assembly pathway of the RP rather than being involved in modulation of proteasomal activities.

Nas6, Nas2, Rpn14, and Hsm3 Are Required for 26S Proteasome Assembly

The above results suggest a functional relationship among the four PIPs (Nas6, Nas2, Rpn14, and Hsm3). To test this, we crossed strains lacking *NAS6*, *NAS2*, *RPN14*, or *HSM3* and generated multiple-deletion strains. Although cells with simultaneous deletions of all the four PIP genes were viable at 25°C, the

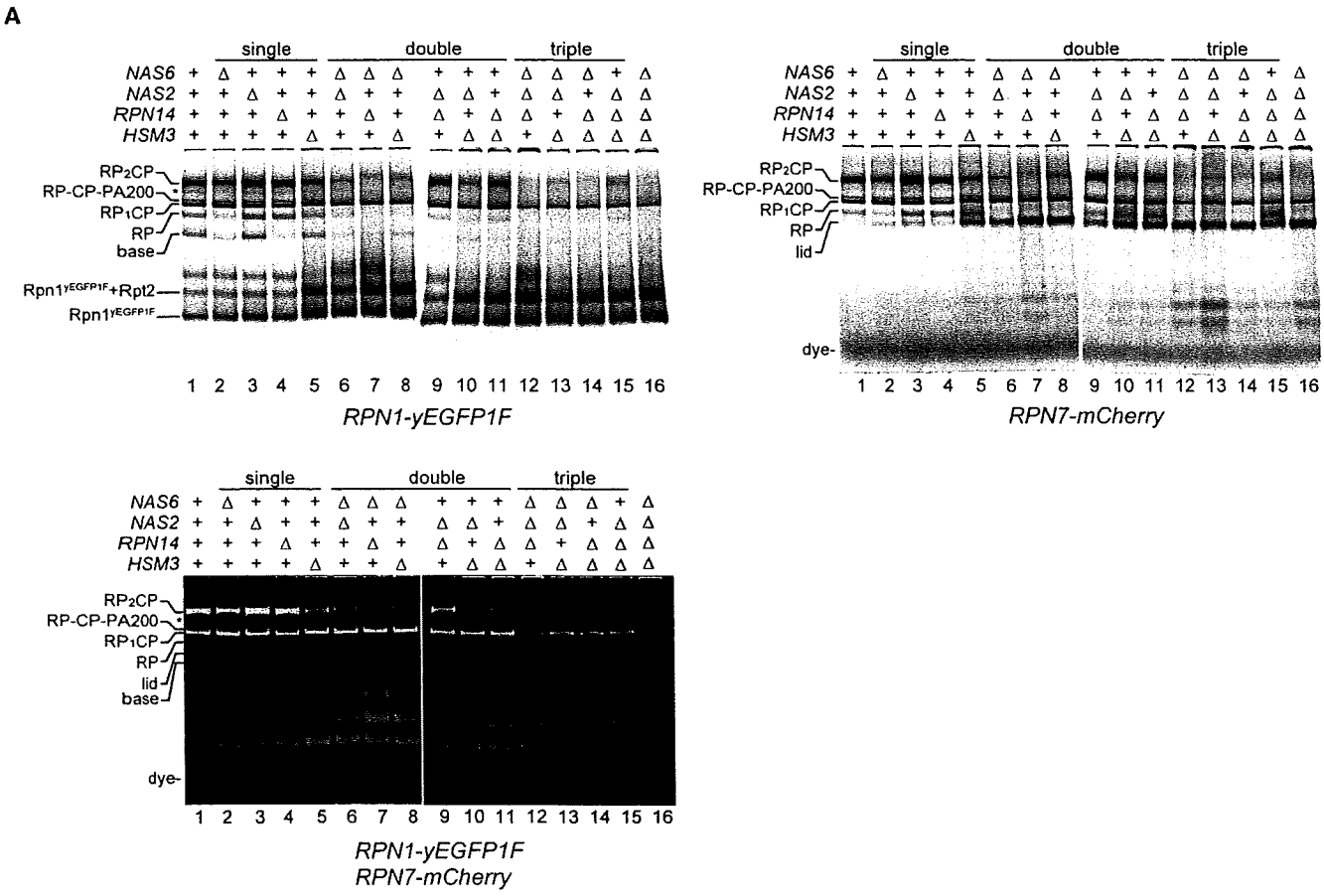

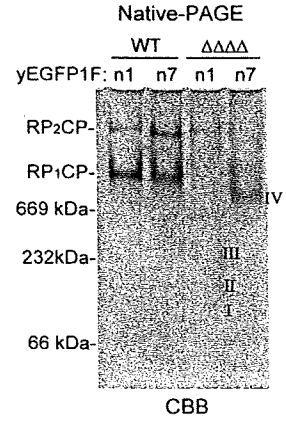

I: Rpn1 (26.5%)
II: Rpn1 (25.9%) + Rpt2 (25.9%)
III: Rpn1 (25.1%) + Rpt2 (20.8%) +Ubp6 (15.2%)

IV: Rpn3 (43.5%) +Rpn5 (43.4%) +Rpn7 (31.5%) Rpn8 (23.7%) +Rpn9 (34.4%) +Rpn11 (39.5%) +Rpn12 (33.9%)

Figure 4. Nas6, Nas2, Rpn14, and Hsm3 Are Important for Base Assembly

(A) Cells expressing Rpn1-yEGFP1F and Rpn7-mCherry (YYS1601-YYS1616) were cultured for 4 hr at 37°C. Extracts were resolved by native-PAGE. Fluorescence of the Rpn1-yEGFP1F (top-left) and Rpn7-mCherry (top-right) were imaged by a fluoroimager. The protein bands assigned to 26S proteasomes (RP_2CP and RP_1CP), RP, base, lid, Rpn1-containing complex ($Rpn1^{yEGFP1F}$-Rpt2 identified in [C]) and free Rpn1 are indicated. The unknown species of the 26S proteasome, probably RP-CP-base, is indicated by an asterisk.

(B) SDS-PAGE analysis of the Rpn1 (n1)- or Rpn7 (n7)-containing complex from *Δnas6 Δnas2 Δrpn14 Δhsm3* (ΔΔΔΔ) cells. Rpn1- and Rpn7-containing complexes were affinity purified from yEGFP1F-tagged cells (YYS1255, 1256, 1258, and 1259).

(C) Identification of subassemblies of the Rpn1- and Rpn7-containing complexes. The purified proteins were resolved on 3.5% native-PAGE followed by Coomassie brilliant blue (CBB) staining. Visible bands were excised, digested with trypsin, and subjected to LC-MSMS. The sequence coverages of the identified proteins are indicated in parenthesis.

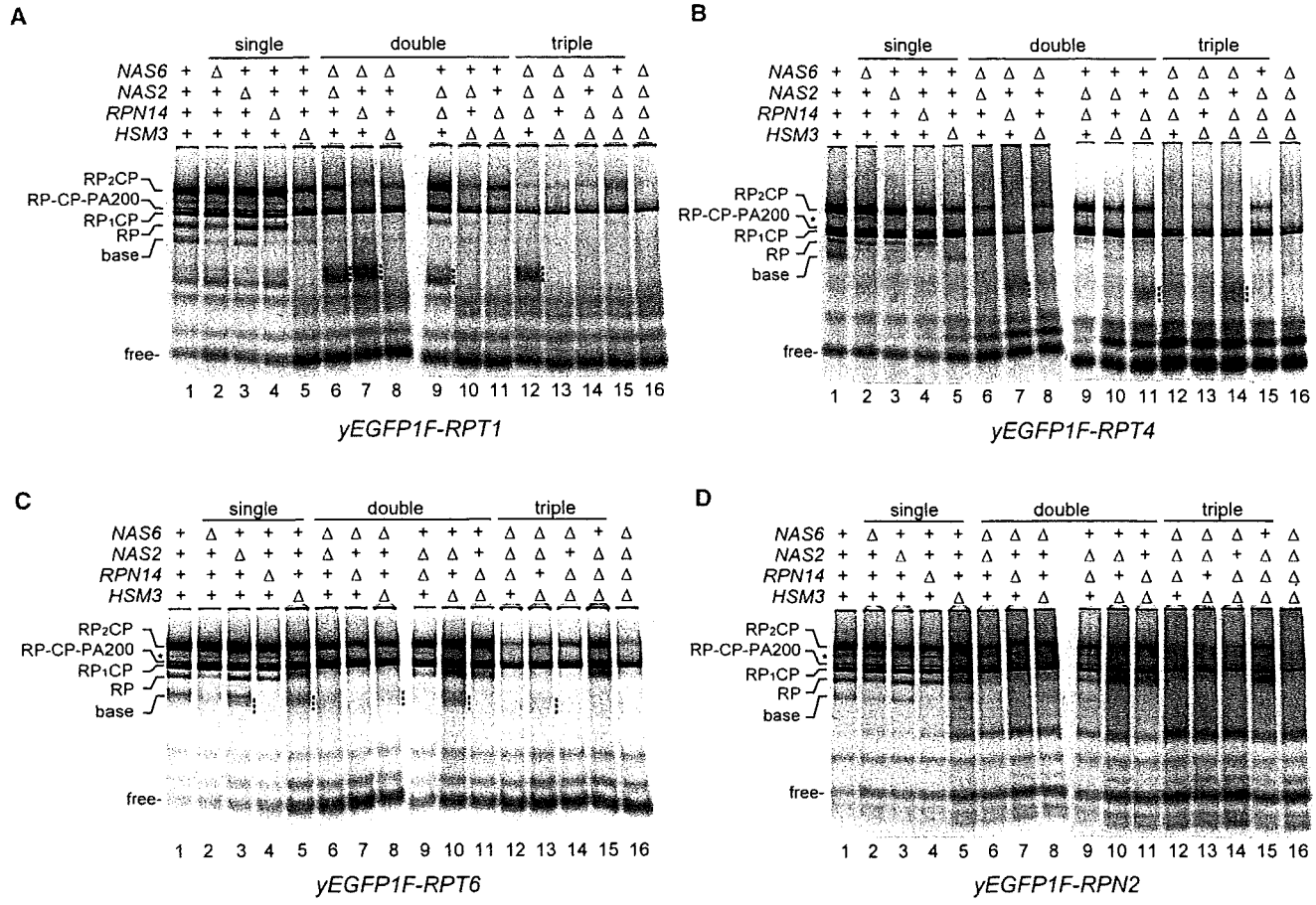

Figure 5. Each Base Chaperone Plays a Distinct Role in Base Assembly

Cells expressing yEGFP1F-Rpt1 ([A], YYS1401-1416), yEGFP1F-Rpt4 ([B], YYS1441-1456), yEGFP1F-Rpt6 ([C], YYS1461-1476), and yEGFP1F-Rpn2 ([D], YYS1501-1516), were cultured and analyzed as in Figure 4A. Characteristic complexes are indicated by dashed lines. See the main text for details.

cells exhibited the most severe growth defects against high temperatures and amino acid-analog stresses among the mutant cells (Figure 3A). The results suggested overlap in the functions of these four PIPs. Furthermore, multiple genetic interactions revealed several hierarchical clusterings within these PIP genes. *Δnas6 Δrpn14* cells and *Δnas2 Δhsm3* cells showed severe growth defect at high temperatures, indicating that each pair (*NAS6-RPN14* and *NAS2-HSM3*) is redundant. In contrast, no genetic interaction was found between *NAS2* and *RPN14*. On the other hand, the triple-mutant *Δnas2 Δrpn14 Δhsm3* cells grew better than the other triple mutants at 33.8°C, suggesting that Nas6 has somehow an overriding function among the four genes.

To determine the functional roles of these four PIPs, we monitored the proteasome assembly by in-gel peptidase assay of total cell extracts. The PIP mutant cells were cultured at 37°C for 4.5 hr, corresponding to two-doubling time, and lysed in the presence of ATP, and then the cleared lysate was resolved by native-PAGE. The activities of the 26S proteasome, RP_2CP and RP_1CP, were visualized with the chromogenic peptide, succinyl-Leu-Leu-Val-Tyr-7-amide-4-methyl-coumarin (Suc-LLVY-AMC), in the presence of ATP (Figure 3B, top panel) after visualization of the latent CP in the presence of a detergent (0.05% SDS) (Figure 3B, bottom panel). Surprisingly, the 26S proteasome was hardly detected in the quadruple, triple, and various double mutants (Figure 3B, top panel). In contrast, the free CP accumulated at high levels in these mutants (Figure 3B, bottom panel), presumably because of a defective RP-CP interaction or RP assembly. These results suggest that one function of the Nas6, Nas2, Rpn14, and Hsm3 is to facilitate the assembly of the 26S proteasome.

Nas6, Nas2, Rpn14, and Hsm3 Are Bona Fide Base Chaperones

We further investigated the mechanism by which Nas6, Nas2, Rpn14, and Hsm3 function in 26S proteasome assembly. To detect the complex at high resolution and with high sensitivity, we used fluorescent protein (FP) imaging, in which the FP-tagged proteins are detected in native-polyacrylamide gel (Lehmann et al., 2008). To monitor the base, lid, RP, and their subassemblies in the same gel, we assayed the total extracts of the Rpn1-yEGFP1F- and Rpn7-mCherry-expressing cells (Figure 4A). Interestingly, multiple species containing Rpn1-yEGFP1F were detected even in the wild-type cell and were assigned to

RP_2CP, RP-CP-PA200, RP_1CP, free RP, free base, and three Rpn1-containing species from top to bottom (Figure 4A, left upper, lane 1). On the other hand, Rpn7-mCherry-containing species were assigned to RP_2CP, RP-CP-PA200, RP_1CP, free RP, and free lid (Figure 4A, right upper, lane 1).

Strikingly, in the quadruple-mutant cells, almost no 26S proteasomes, no free RP, and no free base were detected; instead, only the two small Rpn1-containing species and the free lid accumulated in the cells (Figure 4A, lane 16). To identify the Rpn1- or Rpn7-containing complexes, we performed affinity purification by using the Flag tag of yEGFP1F (Figures 4B). All of the RP subunits were copurified with both the Rpn1- and Rpn7-yEGFP1F from the wild-type cells, whereas only a subset of the RP subunits was copurified from the quadruple mutant (Figure 4B). Further, the proteins were resolved by native-PAGE and visible protein bands were analyzed by LC-MSMS (Figure 4C). The fastest migrating protein band detected in Rpn1-yEGFP1F strains contained only Rpn1 and EGFP (band I), whereas a slower migrating band contained both Rpn1 and Rpt2 (band II). In addition, the faint slowest band contained Rpn1, Rpt2, and Ubp6 (band III). As expected, in the major Rpn7-containing protein band from the quadruple mutant, band IV, we identified eight of the nine lid subunits (Figure 4C, lane 4).

Consistent with our previous report that the lid and base subcomplexes can be assembled independently (Isono et al., 2007), a defective base assembly can be accompanied by the production of a free lid. As judged by the levels of free lid, modest to severe impairment of RP assembly was also observed in the single, double, and triple deletion of the *NAS6*, *NAS2*, *RPN14*, and *HSM3* (Figure 4A). Thus, we conclude that these four PIPs function as chaperones for the base assembly.

Each Base Chaperone Plays a Distinct Role in Base Assembly

The fact that the four base chaperones are structurally distinct and bind specific Rpt subunits (Figure 2A) suggests that each chaperone functions in a distinct step(s) of the base assembly. In support of this notion, accumulation of the Rpn1-Rpt2 was observed in all *HSM3* deleted strains (Figure 4A, lanes 5, 8, 10, 11, 13–16). Conversely, a slower migrating Rpn1-containing complex, probably consisting of Rpn1, Rpt1, and Rpt2, was observed in Hsm3-expressing cells and even in the *Δnas6 Δnas2 Δrpn14* mutant (Figure 4A, lanes 1–4, 6, 7, 9, and 12). To monitor other base subunits, we also chromosomally tagged Rpt1, Rpt4, Rpt6, or Rpn2 with yEGFP1F and subjected it to FP imaging. Multiple species, including small subassemblies, were also detected, similar to the Rpn1-yEGFP1F strain (Figure 5). As expected, a characteristic Rpt1-containing complex (i.e., Rpn1-Rpt1-Rpt2 complex) was detected only in the Hsm3-expressing cells (Figure 5A, dashed line). Thus, these results indicate that Hsm3 assists the incorporation of Rpt1 into the Rpn1-Rpt2 complex.

As for Nas2, the proteasome pattern of the *Δnas2* single mutant was indistinguishable from that of the wild-type strain (Figures 4A and 5A–5D, lane 3). However, accumulation of an Rpt4-containing complex was found in Nas2-expressing cells that lacked other base chaperones (Figure 5B, dashed line). Intriguingly, in both the *Δnas6* and *Δrpn14* single-mutant cells, the levels of free base and/or free RP were lower than those in wild-type cells (Figures 4A and 5A–5D, lanes 2 and 4). Remarkably, accumulation of the Rpt6-containing complex with slower migration was noted in Rpn14-expressing cells that lacked other base chaperones (Figure 5C, dashed line). On the other hand, Nas6-expressing cells showed no accumulation of specific subassemblies but rather a disorganized RP-like complex that contained at least Rpt6, Rpn2, and the lid, with a smear band (Figures 4A, 5C, and 5D, lane 15).

Ordered Assembly of the RP

The above results suggest that the base assembly seemed to start with the formation of a specific pair of the base subunits and that the process involved the base chaperones. If the base assembly was executed in an orderly fashion, each of the base chaperones should function in a stepwise manner, and specific intermediates that consist of the base chaperone and certain base subunits should accumulate in specific mutants. To test this, we first searched for intermediates that accumulate in cells lacking other base chaperone by FP imaging (Figure S2). However, we could not detect obvious chaperone-base intermediates except for Hsm3 (Figure S2). We assumed that the possible intermediates did not focus well in the native-gel, probably because of their structural diversity. In fact, several clear bands were seen, but most Nas6- or Rpn14-containing complexes appeared as smear in the native-gel (Figures 1E and S2). To identify the possible intermediate, we performed affinity purification from the yEGFP1F-tagged base chaperone strains, followed by SDS-PAGE analysis (Figure 6A). Although Nas2 was detected in the RP- and base-bound forms (Figure S2A), only a few protein bands were detected in the Nas2 immunoprecipitates (Figure 6A). Interestingly, protein bands corresponding to all the RP subunits were visible in the Rpn14- and Hsm3-containing complexes, but the protein bands, especially some base subunits, appeared with high intensities (Figure 6A). These observations suggest that the immunoprecipitates contain heterogeneous complexes including the putative intermediates.

To quantify each RP subunit of the intermediates, we performed quantitative MS using stable isotope labeling in culture (SILAC): the *Δlys2* background strains were grown in SILAC medium supplemented with "heavy" lysine, ^{13}C-Lys. To prepare isotope-labeled RP that contained all the subunits stoichiometrically, we cultured the *PRE5-3xFLAGΔlys2* cells, in which the CP subunit Pre5 was tagged with 3xFLAG tag, in SILAC medium and captured the 26S proteasome by anti-Flag agarose, and then eluted the RP with high salt-containing buffer (Saeki et al., 2000). Mixtures of each base chaperone-containing complexes and the isotope-labeled RP were digested with lysil endopeptidase in solution and then subjected to LC-MSMS (Figure 6B). Quantitative MS analysis allows determination of the precise amount of each RP subunits even in the heterogeneous complexes. The immunoprecipitates were also subjected to native-PAGE, and visible protein bands were identified by LC-MSMS (Figure 6B).

The major Nas2 complex was Nas2-Rpt4-Rpt5, which was also identified by native-PAGE-MS (Figure 6C). In addition,

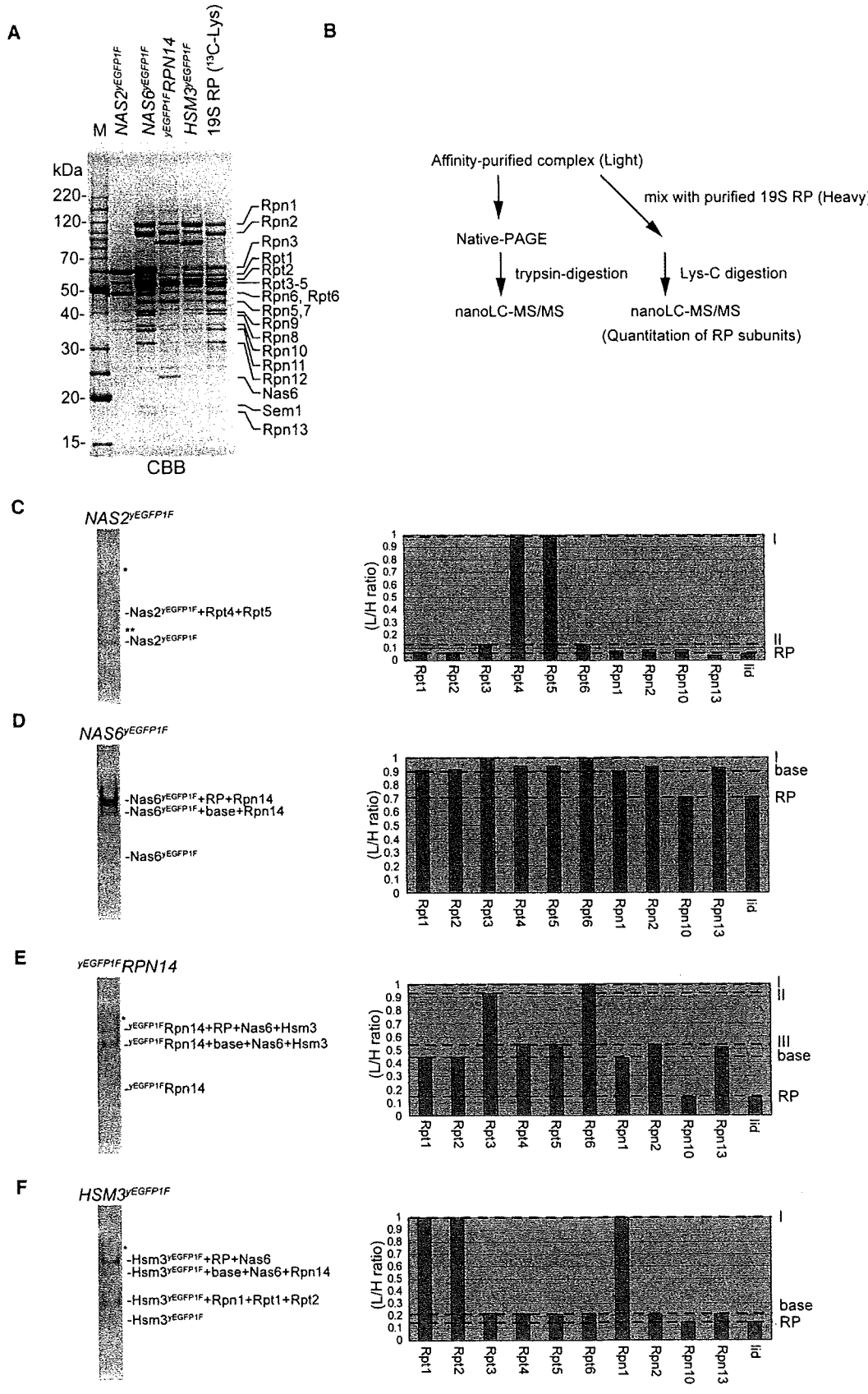
A
M
NAS2yEGFP1F
NAS6yEGFP1F
yEGFP1FRPN14
HSM3yEGFP1F
19S RP (13C-Lys)
kDa
220-
120-
70-
50-
40-
30-
20-
15-
CBB
Rpn1
Rpn2
Rpn3
Rpt1
Rpt2
Rpt3-5
Rpn6, Rpt6
Rpn5,7
Rpn9
Rpn8
Rpn10
Rpn11
Rpn12
Nas6
Sem1
Rpn13
B
Affinity-purified complex (Light)
mix with purified 19S RP (Heavy)
Native-PAGE
trypsin-digestion
Lys-C digestion
nanoLC-MS/MS
nanoLC-MS/MS
(Quantitation of RP subunits)
C
NAS2yEGFP1F
-Nas2yEGFP1F+Rpt4+Rpt5
-Nas2yEGFP1F
(L/H ratio)
I
II
RP
Rpt1
Rpt2
Rpt3
Rpt4
Rpt5
Rpt6
Rpn1
Rpn2
Rpn10
Rpn13
lid
D
NAS6yEGFP1F
-Nas6yEGFP1F+RP+Rpn14
-Nas6yEGFP1F+base+Rpn14
-Nas6yEGFP1F
I
base
RP
E
yEGFP1FRPN14
-yEGFP1FRpn14+RP+Nas6+Hsm3
-yEGFP1FRpn14+base+Nas6+Hsm3
-yEGFP1FRpn14
II
III
base
RP
F
HSM3yEGFP1F
-Hsm3yEGFP1F+RP+Nas6
-Hsm3yEGFP1F+base+Nas6+Rpn14
-Hsm3yEGFP1F+Rpn1+Rpt1+Rpt2
-Hsm3yEGFP1F
I
base
RP

a small amount of the lid subcomplex, 4%–5% of the total Nas2-bound complexes, was detected by MS, suggesting that a small population of Nas2 binds with the RP, until completion of the RP assembly. In contrast, the Nas6 complexes could be divided into two main parts; ~70% was Nas6-RP and ~20% was Nas6-base (Figure 6D). The remaining ~10% of the total complex was Nas6-Rpt3-Rpt6 and a more heterogeneous complex. Interestingly, the Rpn14 complexes were divided into four distinct complexes by MS, Rpn14-Rpt3-Rpt6, Rpn14-Rpt3~Rpt6-Rpn2-Rpn13, Rpn14-base, and Rpn14-RP (Figure 6E). Although the latter two complexes were easily detected by the native-PAGE analysis, the former two were not. These observations add support to our assumption above. On the other hand, three distinct Hsm3 complexes were identified by both the native-PAGE-MS and quantitative MS: Hsm3-Rpt1-Rpt2-Rpn1, Hsm3-base, and Hsm3-RP (Figure 6F). The results of quantitative MS analysis indicate that the base assembly seemed to be executed in a highly orderly fashion, beginning with the formation of the base subunit-chaperone pairs (Figure 7B; see the Discussion).

The Base Chaperones Regulate the Newly Synthesized Subunits

Why didn't the base chaperone-lacking cells show any growth defect at permissive temperatures, considering that the 26S proteasome is essential for cell growth (Figure 3A)? To address the question, we compared the proteasome profiles at permissive temperatures with those at restrictive temperatures. The wild-type or the base chaperone quadruple-mutant cells expressing Rpn1-yEGFP1F were analyzed by FP imaging and in-gel peptidase assay (Figure 7A). In the quadruple-mutant cells, faint signals of 26S proteasome activities were detected in cells cultured at 25°C, while the 26S proteasomes completely disappeared upon a shift to 37°C for 4 hr, corresponding to two doubling time. Interestingly, in the quadruple-mutant cells, formation of RP was noticeable at 25°C, and it converted subsequently into the 26S proteasome after heat shift (Figure 7A). These results suggest that the observed RP is a functional species, but the RP assembly did not proceed without the base chaperones at the restrictive temperature. In contrast, the 26S proteasome in the wild-type cells did not show any obvious changes at both temperatures, suggesting that the base chaperones work to maintain the RP levels in growing cells. During treatment of cells with cyclohexamide (CHX), by which the cell growth was stopped, the dynamic changes in the proteasome profiles were not observed (Figure 7A). Considered together, these results suggest that the base chaperones regulate assembly of the newly synthesized base subunits.

DISCUSSION

The base subcomplex contains six paralogous Rpt subunits and three Rpn subunits (Leggett et al., 2005; Murata et al., 2009). How do the nine different subunits assemble in the base? In the assembly pathway of the CP, two dimeric chaperones, PAC1-2 and PAC3-4, arrange the seven α-subunits into defined positions in the α-ring (Kusmierczyk and Hochstrasser, 2008; Murata et al., 2009; Ramos and Dohmen, 2008). Because the six ATPases of the base are thought to form a ring structure like the CP α-ring, it is reasonable to suppose that specific factors may help the base assembly.

In this study, we identified four proteasome-interacting proteins, Nas2, Nas6, Rpn14, and Hsm3, as plausible chaperones for the base assembly; (1) absence of these PIPs caused the defect of the base assembly, (2) each PIP specifically binds its partner Rpt subunit and forms a distinct subassembly of the base, and (3) none of these PIPs are present in the 26S proteasome. Because each base chaperone has a distinct structure, it was surprising that they function in the same pathway. Our conclusions regarding Nas2/p27 and Hsm3/S5b are consistent with those of a previous report that both p27 and S5b can form specific subassemblies (DeMartino et al., 1996; Deveraux et al., 1995). As for Nas6/gankyrin and Rpn14/PAAF1, our genetic study clearly suggests that these proteins functions in the base assembly, contrary to previous observations in mammalian cells (Dawson et al., 2002; Higashitsuji et al., 2000; Lassot et al., 2007; Park et al., 2005). Possibly, mammalian gankyrin and PAAF1 may have species-specific functions, although either gankyrin or PAAF1 could suppress the temperature sensitivity of the *Δnas6 Δrpn14* strain (data not shown). During the preparation of this manuscript, Le Tallec et al. also identified Hsm3/S5b as a base chaperone in an elegant genetic screening study (Le Tallec et al., 2009). As evident from the results of the present study, Hsm3 is only part of a larger group of chaperones that are required for the orderly process of base assembly (Figures 3–7).

Base Chaperones Regulate the Highly Structured Assembly of the 19S Regulatory Particle

Our Y2H and quantitative MS analyses identified the mechanisms involved in the base assembly (Figures 2 and 6). The

Figure 6. Quantitation of the Base Chaperone-RP Subunit Intermediates by MS

(A) SDS-PAGE analysis of the base chaperone-containing complexes. Affinity-purified proteins from the respective yEGFP1F-tagged strains (YYS1541, 1591, 1621, 1631) were subjected to SDS-PAGE followed by CBB staining. As a control, the isotopically labeled RP (^{13}C-Lys) was also prepared from the *PRE5-3xFLAG* strain (YYS1297). Protein bands corresponding to the bait protein are indicated by red asterisks. In the case of *NAS2-yEGFP1F*, an N-terminally truncated form of Nas2 is also identified by MS.

(B) Depiction of overall workflow.

(C–F) Left panels: Identification of the base chaperone-RP subunit intermediates by native-PAGE. The affinity-purified proteins in (A) were resolved in 3.5% native-PAGE, followed by CBB staining. Visible protein bands were analyzed by LC-MSMS. Contaminant proteins, identified as ribosomal proteins, are indicated by asterisks. From the band with relatively high intensity indicated by the double asterisk, only Nas2-yEGFP1F was identified. Right panels: Quantitation of the base chaperone-bound RP subunits. The affinity-purified proteins in (A) were mixed with the isotope-labeled RP and analyzed by LC-MSMS. The relative amounts of the RP subunits were determined by comparison of the intensities of multiple SILAC ion pairs (light [L] versus heavy [H] ions). The L/H ratios of each RP subunits are shown with mean values of three experiments in the graph (SD < 0.05). Because the L/H ratios of all nine lid subunits were essentially of the same value, we simply note the lid. Multiple complexes were ranked by the relative levels and are indicated by dashed red line.

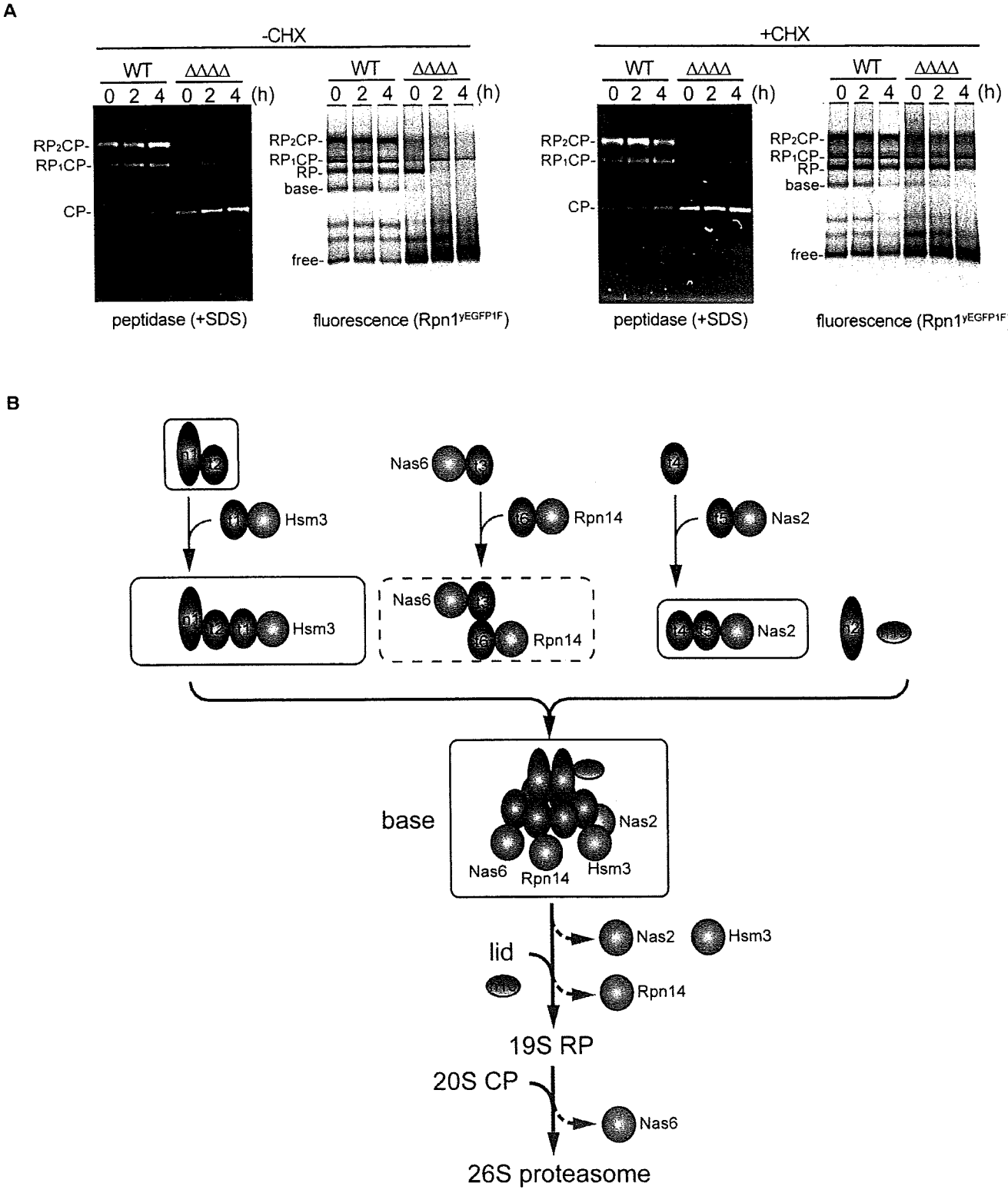

Figure 7. The Assembly Pathway of the RP by Base Chaperones

(A) Base chaperones regulate newly synthesized proteasomes. Wild-type (WT) or *Δnas6 Δnas2 Δrpn14 Δhsm3* (ΔΔΔΔ) cells expressing Rpn1-yEGFP1F (YYS1255 or 1258) were cultured at 25°C, then shifted at 37°C for 2–4 hr. Proteasomes were imaged as in Figures 3B and 4A. As a control, cyclohexamide (+CHX, 400 μg/ml) was added before the heat shift.

base assembly seems to begin with the formation of specific complexes between the Rpt subunit and base chaperones such as Rpt1-Hsm3, Rpt3-Nas6, Rpt5-Nas2, and Rpt6-Rpn14, followed by the formation of relatively stable intermediates: Rpn1-Rpt2-Rpt1-Hsm3, Rpt4-Rpt5-Nas2, and Nas6-Rpt3-Rpt6-Rpn14. Subsequently, all intermediates and the remaining base subunits, Rpn2 and Rpn13, are assembled to form the base subcomplex (see the model illustrated in Figure 7B). After the completion of the base assembly, the base binds the lid and Rpn10 and forms the 19S RP (Figure 7B).

Because *NAS6* and *RPN14* are epistatic to *NAS2* and *HSM3* (Figure 3A), the Nas6-Rpt3-Rpt6-Rpn14 complex might serve as the seed for the base assembly. Although Nas2 might function in the incorporation of Rpt4-Rpt5 into the base, the proteasome profiles in the *Δnas2* strain were essentially the same as that of wild-type strain (Figures 4 and 5). The incorporation of Rpt4-Rpt5 might occur spontaneously or might not be the limiting step in the assembly in the *Δnas2* cells. Nevertheless, our genetic study suggests that *NAS2* is indispensable when lacking other base chaperones (Figure 3A).

The mechanism for how each base chaperones is released remains unclear. Although all the base chaperones seemed to associate with the base and RP, their binding properties were somehow different (Figures 6 and S2). Only a small fraction of Nas2 and Hsm3 is associated with base and completed RP. On the other hand, Nas6 was associated with both the base and RP, whereas Rpn14 is associated mainly with the base. It is likely that the completion of base assembly may stimulate Nas2 and Hsm3 release and that the lid-binding may stimulate Rpn14 displacement. Finally, Nas6 is released upon the CP binding (Figure 7B). Further studies, such as a reconstitution assay using purified proteins or structural studies, are needed to solve the precise mechanisms of action of the base chaperones.

At present, there is little information on the assembly of the lid subcomplex. Consistent with the finding of a previous report (Isono et al., 2007), the lid assembly appears to occur independently of the base assembly (Figures 4 and 5). Although Hsp90 chaperone seemed to be involved in this process (Imai et al., 2003), more specific lid-dedicated chaperones may still exist. Finally, Rpn10, which stabilizes the lid-base interaction (Glickman et al., 1998), is apparently incorporated into the RP, probably after the lid-base binding (Figure 7B).

Biological Significance of the Base Chaperones

Although loss of the base chaperones resulted in significant reductions in 26S proteasome levels, the quadruple-mutant cells grow normally under normal conditions (Figures 3A and 7A). The result suggests that alternative mechanism(s) for the base assembly, though it seems to be ineffective, still exists in the cells. For example, it has been proposed that the CP itself, probably the α ring, functions as an assembly factor for the base assembly (Kusmierczyk et al., 2008). Likewise, the lid subcomplex may act as a scaffold for the base assembly, although these subcomplexes can be formed independently (Isono et al., 2007). Alternatively, the base subunits may have intrinsic ability to form the base subcomplex spontaneously.

Under urgent conditions that require 26S proteasome activity, such as heat stress, the base chaperones are indispensable in the maintenance of the amount of the 26S proteasome at levels sufficient for cell viability (Figure 3A). It should be noted that the protein levels of the base chaperones are at least 20-fold lower than the integral proteasome subunits (Ghaemmaghami et al., 2003), suggesting that the base chaperones exert the complicated task to maintain 26S proteasome levels as needed.

EXPERIMENTAL PROCEDURES

Yeast Strains, Plasmids, and Media

For descriptions of yeast strains, plasmids, and media, see the Supplemental Experimental Procedures.

Protein Purification and Mass Spectrometry

Affinity purifications of the 3xFlag- or yEGFP1F-tagged PIP complexes were performed essentially as described for the preparation of the 26S yeast proteasome (Saeki et al., 2005). In brief, cell extract prepared in the presence of ATP and the FLAG-tagged protein was recovered by adsorption to an anti-FLAG M2 agarose (Sigma), followed by elution with 3xFLAG peptide. Protein samples were analyzed by LC-coupled MALDI-TOF mass spectrometry with a 4800 MALDI TOF/TOF analyzer (Applied Biosystems, Foster City, CA) coupled with DiNA MaP system (KYA tech, Japan) as described previously (Saeki et al., 2009; Tanaka et al., 2008). For quantitative MS analysis, proteins were denatured with 0.5% RapiGest (Waters) in 50 mM Tris-HCl (pH 8.8) and digested with 100 ng/μl lysil endopeptidase (Wako) for 16 hr at 37°C. The resulting peptides were subjected to LC-MALD. MS and MS/MS data were processed by ProteinPilot software 2.0 (Applied Biosystems).

Microscopy

Cells that chromosomally expressed the yEGFP1F- and/or mCherry-tagged proteins were grown in YPD medium to logarithmic phase at 25°C. Then they were washed twice with phosphate buffered saline and imaged with a BX52 fluorescence microscope (Olympus, Tokyo) with a UPlanApo 100×/1.45 objective (Olympus) equipped with a confocal scanner unit CSU20 (Yokogawa Electric, Japan) and a C9100 EMCCD camera (Hamamatsu Photonics) as described previously (Isono et al., 2007).

Native-PAGE and Fluorescent Imaging

The cells were disrupted with glass beads as described previously (Saeki et al., 2005). The lysates were clarified by centrifugation at 15,000 rpm for 5 min at 2°C, and the supernatants were further centrifuged at 15,000 rpm for 15 min at 2°C. The resultant supernatant (30 μg, typically 3 μl) was mixed with 4× native sample buffer and then subjected to 3.5% native-PAGE, unless otherwise noted (Elsasser et al., 2005). For the FP imaging, the gel was poured in nonluminescent glass plates (Biocraft, Japan). After electrophoresis, FP fluorescence was imaged by a Typhoon9400 fluoroimager (GE Healthcare Biosciences, Uppsala, Sweden). In-gel peptidase assay was performed as described previously (Saeki et al., 2009).

Western Blotting

Western blotting was performed as described previously (Saeki et al., 2005) with the following antibodies: horseradish peroxidase-conjugated anti-Flag antibody (M2, Sigma), anti-ubiquitin antibody (P4D1, Santa Cruz Biotechnology, Santa Cruz, CA), anti-Rpt5 antibody (Affiniti Research), anti-Rpn5 antibody (Isono et al., 2007), and anti-CP antibody (Tanaka et al., 1988).

(B) Current model for the assembly pathway of the yeast RP. The intermediates identified by native-PAGE-MS are indicated in green box. The intermediates identified by the quantitative MS are boxed in green dotted line. Note that Rpn and Rpt subunits are abbreviated as "n" and "t," respectively. See the main text for details.

SUPPLEMENTAL DATA

Supplemental Data include Supplemental Experimental Procedures and two figures and can be found with this article online at http://www.cell.com/supplemental/S0092-8674(09)00528-5.

ACKNOWLEDGMENTS

The authors thank B.P. Cormack for kindly providing the yEGFP1 plasmid. We are grateful to all members of K.T.'s laboratory for the useful discussions. This work was supported by grants from the Ministry of Education, Science, Sports, Culture, and Technology (MEXT) of Japan (to A.T. and K.T.) and the Target Protein Project of MEXT (Y.S. and K.T.).

Received: March 23, 2009
Revised: April 27, 2009
Accepted: May 1, 2009
Published online: May 14, 2009

REFERENCES

Baumeister, W., Walz, J., Zuhl, F., and Seemuller, E. (1998). The proteasome: paradigm of a self-compartmentalizing protease. Cell *92*, 367–380.

Coux, O., Tanaka, K., and Goldberg, A.L. (1996). Structure and functions of the 20S and 26S proteasomes. Annu. Rev. Biochem. *65*, 801–847.

Dawson, S., Apcher, S., Mee, M., Higashitsuji, H., Baker, R., Uhle, S., Dubiel, W., Fujita, J., and Mayer, R.J. (2002). Gankyrin is an ankyrin-repeat oncoprotein that interacts with CDK4 kinase and the S6 ATPase of the 26 S proteasome. J. Biol. Chem. *277*, 10893–10902.

DeMartino, G.N., Proske, R.J., Moomaw, C.R., Strong, A.A., Song, X., Hisamatsu, H., Tanaka, K., and Slaughter, C.A. (1996). Identification, purification, and characterization of a PA700-dependent activator of the proteasome. J. Biol. Chem. *271*, 3112–3118.

Deveraux, Q., Jensen, C., and Rechsteiner, M. (1995). Molecular cloning and expression of a 26 S protease subunit enriched in dileucine repeats. J. Biol. Chem. *270*, 23726–23729.

Elsasser, S., Schmidt, M., and Finley, D. (2005). Characterization of the proteasome using native gel electrophoresis. Methods Enzymol. *398*, 353–363.

Enenkel, C., Lehmann, A., and Kloetzel, P.M. (1998). Subcellular distribution of proteasomes implicates a major location of protein degradation in the nuclear envelope-ER network in yeast. EMBO J. *17*, 6144–6154.

Fatica, A., Oeffinger, M., Dlakic, M., and Tollervey, D. (2003). Nob1p is required for cleavage of the 3′ end of 18S rRNA. Mol. Cell. Biol. *23*, 1798–1807.

Fedorova, I.V., Gracheva, L.M., Kovaltzova, S.V., Evstuhina, T.A., Alekseev, S.Y., and Korolev, V.G. (1998). The yeast HSM3 gene acts in one of the mismatch repair pathways. Genetics *148*, 963–973.

Fedorova, I.V., Kovaltzova, S.V., Gracheva, L.M., Evstuhina, T.A., and Korolev, V.G. (2004). Requirement of HSM3 gene for spontaneous mutagenesis in Saccharomyces cerevisiae. Mutat. Res. *554*, 67–75.

Ghaemmaghami, S., Huh, W.K., Bower, K., Howson, R.W., Belle, A., Dephoure, N., O'Shea, E.K., and Weissman, J.S. (2003). Global analysis of protein expression in yeast. Nature *425*, 737–741.

Gillette, T.G., Kumar, B., Thompson, D., Slaughter, C.A., and DeMartino, G.N. (2008). Differential roles of the COOH termini of AAA subunits of PA700 (19 S regulator) in asymmetric assembly and activation of the 26 S proteasome. J. Biol. Chem. *283*, 31813–31822.

Glickman, M.H., Rubin, D.M., Coux, O., Wefes, I., Pfeifer, G., Cjeka, Z., Baumeister, W., Fried, V.A., and Finley, D. (1998). A subcomplex of the proteasome regulatory particle required for ubiquitin-conjugate degradation and related to the COP9-signalosome and eIF3. Cell *94*, 615–623.

Hanna, J., and Finley, D. (2007). A proteasome for all occasions. FEBS Lett. *581*, 2854–2861.

Hershko, A., and Ciechanover, A. (1998). The ubiquitin system. Annu. Rev. Biochem. *67*, 425–479.

Higashitsuji, H., Itoh, K., Nagao, T., Dawson, S., Nonoguchi, K., Kido, T., Mayer, R.J., Arii, S., and Fujita, J. (2000). Reduced stability of retinoblastoma protein by gankyrin, an oncogenic ankyrin-repeat protein overexpressed in hepatomas. Nat. Med. *6*, 96–99.

Hori, T., Kato, S., Saeki, M., DeMartino, G.N., Slaughter, C.A., Takeuchi, J., Toh-e, A., and Tanaka, K. (1998). cDNA cloning and functional analysis of p28 (Nas6p) and p40.5 (Nas7p), two novel regulatory subunits of the 26S proteasome. Gene *216*, 113–122.

Imai, J., Maruya, M., Yashiroda, H., Yahara, I., and Tanaka, K. (2003). The molecular chaperone Hsp90 plays a role in the assembly and maintenance of the 26S proteasome. EMBO J. *22*, 3557–3567.

Isono, E., Nishihara, K., Saeki, Y., Yashiroda, H., Kamata, N., Ge, L., Ueda, T., Kikuchi, Y., Tanaka, K., Nakano, A., and Toh-e, A. (2007). The assembly pathway of the 19S regulatory particle of the yeast 26S proteasome. Mol. Biol. Cell *18*, 569–580.

Kusmierczyk, A.R., and Hochstrasser, M. (2008). Some assembly required: dedicated chaperones in eukaryotic proteasome biogenesis. Biol. Chem. *389*, 1143–1151.

Kusmierczyk, A.R., Kunjappu, M.J., Funakoshi, M., and Hochstrasser, M. (2008). A multimeric assembly factor controls the formation of alternative 20S proteasomes. Nat. Struct. Mol. Biol. *15*, 237–244.

Lassot, I., Latreille, D., Rousset, E., Sourisseau, M., Linares, L.K., Chable-Bessia, C., Coux, O., Benkirane, M., and Kiernan, R.E. (2007). The proteasome regulates HIV-1 transcription by both proteolytic and nonproteolytic mechanisms. Mol. Cell *25*, 369–383.

Le Tallec, B., Barrault, M.B., Guerois, R., Carre, T., and Peyroche, A. (2009). Hsm3/S5b participates in the assembly pathway of the 19S regulatory particle of the proteasome. Mol. Cell *33*, 389–399.

Leggett, D.S., Hanna, J., Borodovsky, A., Crosas, B., Schmidt, M., Baker, R.T., Walz, T., Ploegh, H., and Finley, D. (2002). Multiple associated proteins regulate proteasome structure and function. Mol. Cell *10*, 495–507.

Leggett, D.S., Glickman, M.H., and Finley, D. (2005). Purification of proteasomes, proteasome subcomplexes, and proteasome-associated proteins from budding yeast. Methods Mol. Biol. *301*, 57–70.

Lehmann, A., Jechow, K., and Enenkel, C. (2008). Blm10 binds to pre-activated proteasome core particles with open gate conformation. EMBO Rep. *9*, 1237–1243.

Lozano, G., and Zambetti, G.P. (2005). Gankyrin: an intriguing name for a novel regulator of p53 and RB. Cancer Cell *8*, 3–4.

Murata, S., Yashiroda, H., and Tanaka, K. (2009). Molecular mechanisms of proteasome assembly. Nat. Rev. Mol. Cell Biol. *10*, 104–115.

Nakamura, Y., Nakano, K., Umehara, T., Kimura, M., Hayashizaki, Y., Tanaka, A., Horikoshi, M., Padmanabhan, B., and Yokoyama, S. (2007a). Structure of the oncoprotein gankyrin in complex with S6 ATPase of the 26S proteasome. Structure *15*, 179–189.

Nakamura, Y., Umehara, T., Tanaka, A., Horikoshi, M., Padmanabhan, B., and Yokoyama, S. (2007b). Structural basis for the recognition between the regulatory particles Nas6 and Rpt3 of the yeast 26S proteasome. Biochem. Biophys. Res. Commun. *359*, 503–509.

Park, Y., Hwang, Y.P., Lee, J.S., Seo, S.H., Yoon, S.K., and Yoon, J.B. (2005). Proteasomal ATPase-associated factor 1 negatively regulates proteasome activity by interacting with proteasomal ATPases. Mol. Cell. Biol. *25*, 3842–3853.

Pickart, C.M., and Cohen, R.E. (2004). Proteasomes and their kin: proteases in the machine age. Nat. Rev. Mol. Cell Biol. *5*, 177–187.

Rabl, J., Smith, D.M., Yu, Y., Chang, S.C., Goldberg, A.L., and Cheng, Y. (2008). Mechanism of gate opening in the 20S proteasome by the proteasomal ATPases. Mol. Cell *30*, 360–368.

Ramos, P.C., and Dohmen, R.J. (2008). PACemakers of proteasome core particle assembly. Structure *16*, 1296–1304.

Rencus-Lazar, S., Amir, Y., Wu, J., Chien, C.T., Chamovitz, D.A., and Segal, D. (2008). The proto-oncogene Int6 is essential for neddylation of Cul1 and Cul3 in Drosophila. PLoS ONE *3*, e2239.

Russell, S.J., Steger, K.A., and Johnston, S.A. (1999). Subcellular localization, stoichiometry, and protein levels of 26 S proteasome subunits in yeast. J. Biol. Chem. *274*, 21943–21952.

Saeki, Y., Toh-e, A., and Yokosawa, H. (2000). Rapid isolation and characterization of the yeast proteasome regulatory complex. Biochem. Biophys. Res. Commun. *273*, 509–515.

Saeki, Y., Isono, E., and Toh-e, A. (2005). Preparation of ubiquitinated substrates by the PY motif-insertion method for monitoring 26S proteasome activity. Methods Enzymol. *399*, 215–227.

Saeki, Y., Kudo, T., Sone, T., Kikuchi, Y., Yokosawa, H., Toh-e, A., and Tanaka, K. (2009). Lysine 63-linked polyubiquitin chain may serve as a targeting signal for the 26S proteasome. EMBO J. *28*, 359–371.

Samanta, M.P., and Liang, S. (2003). Predicting protein functions from redundancies in large-scale protein interaction networks. Proc. Natl. Acad. Sci. USA *100*, 12579–12583.

Schwartz, A.L., and Ciechanover, A. (2009). Targeting proteins for destruction by the ubiquitin system: implications for human pathobiology. Annu. Rev. Pharmacol. Toxicol. *49*, 73–96.

Seong, K.M., Baek, J.H., Yu, M.H., and Kim, J. (2007). Rpn13p and Rpn14p are involved in the recognition of ubiquitinated Gcn4p by the 26S proteasome. FEBS Lett. *581*, 2567–2573.

Smith, D.M., Chang, S.C., Park, S., Finley, D., Cheng, Y., and Goldberg, A.L. (2007). Docking of the proteasomal ATPases' carboxyl termini in the 20S proteasome's alpha ring opens the gate for substrate entry. Mol. Cell *27*, 731–744.

Takeuchi, J., Fujimuro, M., Yokosawa, H., Tanaka, K., and Toh-e, A. (1999). Rpn9 is required for efficient assembly of the yeast 26S proteasome. Mol. Cell. Biol. *19*, 6575–6584.

Tanaka, K., Yoshimura, T., Kumatori, A., Ichihara, A., Ikai, A., Nishigai, M., Kameyama, K., and Takagi, T. (1988). Proteasomes (multi-protease complexes) as 20 S ring-shaped particles in a variety of eukaryotic cells. J. Biol. Chem. *263*, 16209–16217.

Tanaka, Y., Tanaka, N., Saeki, Y., Tanaka, K., Murakami, M., Hirano, T., Ishii, N., and Sugamura, K. (2008). c-Cbl-dependent monoubiquitination and lysosomal degradation of gp130. Mol. Cell. Biol. *28*, 4805–4818.

Tone, Y., and Toh-e, A. (2002). Nob1p is required for biogenesis of the 26S proteasome and degraded upon its maturation in Saccharomyces cerevisiae. Genes Dev. *16*, 3142–3157.

Verma, R., Chen, S., Feldman, R., Schieltz, D., Yates, J., Dohmen, J., and Deshaies, R.J. (2000). Proteasomal proteomics: identification of nucleotide-sensitive proteasome-interacting proteins by mass spectrometric analysis of affinity-purified proteasomes. Mol. Biol. Cell *11*, 3425–3439.

Watanabe, T.K., Saito, A., Suzuki, M., Fujiwara, T., Takahashi, E., Slaughter, C.A., DeMartino, G.N., Hendil, K.B., Chung, C.H., Tanahashi, N., and Tanaka, K. (1998). cDNA cloning and characterization of a human proteasomal modulator subunit, p27 (PSMD9). Genomics *50*, 241–250.

Wendler, P., Lehmann, A., Janek, K., Baumgart, S., and Enenkel, C. (2004). The bipartite nuclear localization sequence of Rpn2 is required for nuclear import of proteasomal base complexes via karyopherin alphabeta and proteasome functions. J. Biol. Chem. *279*, 37751–37762.

Yahalom, A., Kim, T.H., Roy, B., Singer, R., von Arnim, A.G., and Chamovitz, D.A. (2008). Arabidopsis eIF3e is regulated by the COP9 signalosome and has an impact on development and protein translation. Plant J. *53*, 300–311.

Yen, H.C., and Chang, E.C. (2003). INT6–a link between the proteasome and tumorigenesis. Cell Cycle *2*, 81–83.

Cell

Assembly Pathway of the Mammalian Proteasome Base Subcomplex Is Mediated by Multiple Specific Chaperones

Takeumi Kaneko,[1] Jun Hamazaki,[1] Shun-ichiro Iemura,[2] Katsuhiro Sasaki,[3] Kaori Furuyama,[1] Tohru Natsume,[2] Keiji Tanaka,[3] and Shigeo Murata[1,*]

[1]Laboratory of Protein Metabolism, Graduate School of Pharmaceutical Sciences, The University of Tokyo, 7-3-1 Hongo, Bunkyo-ku, Tokyo 113-0033, Japan

[2]National Institute of Advanced Industrial Science and Technology, Biological Information Research Center, 2-42 Aomi, Kohtoh-ku, Tokyo 135-0064, Japan

[3]Laboratory of Frontier Science, Core Technology and Research Center, Tokyo Metropolitan Institute of Medical Science, 2-1-6 Kamikitazawa, Setagaya-ku, Tokyo 156-8506, Japan

*Correspondence: smurata@mol.f.u-tokyo.ac.jp

DOI 10.1016/j.cell.2009.05.008

SUMMARY

The 26S proteasome is an enzymatic complex that degrades ubiquitinated proteins in eukaryotic cells. It is composed of the 20S core particle (CP) and the 19S regulatory particle (RP). The latter is further divided into the lid and base subcomplexes. While the mechanism involved in the assembly of the CP is well investigated, that of the RP is poorly understood. Here, we show that the formation of the mammalian base subcomplex involves three distinct modules, where specific pairs of ATPase subunits are associated with the distinct chaperones p28, S5b, or p27. The process of base formation starts from association of the p28-Rpt3-Rpt6-Rpn14 complex with the S5b-Rpt1-Rpt2-Rpn1 complex, followed by incorporation of the p27-Rpt5-Rpt4 complex and Rpn2, where p28, S5b, and p27 regulate the associations between the modules. These chaperones dissociate before completion of 26S proteasome formation. Our results demonstrate that base assembly is facilitated by multiple proteasome-dedicated chaperones, like CP assembly.

INTRODUCTION

The 26S proteasome is a eukaryotic ATP-dependent protease responsible for the degradation of proteins tagged with polyubiquitin chains (Coux et al., 1996; Hershko and Ciechanover, 1998). The ubiquitin-dependent proteolysis by the proteasome serves a diverse array of cellular processes including cell-cycle regulation, DNA repair, apoptosis, signal transduction, and protein quality control by catalyzing selective degradation of short-lived regulatory proteins and damaged proteins (Ravid and Hochstrasser, 2008; Schwartz and Ciechanover, 2009).

The 26S proteasome is a large protein complex composed of the catalytic 20S core particle (CP; also called the 20S proteasome) and the 19S regulatory particle (RP; also called PA700 in mammals), which is attached to either or both ends of the CP. The CP is a cylindrical shaped stack of four heptameric rings, where the outer rings and inner rings are each composed of seven homologous α subunits (α1–α7) and seven homologous β subunits (β1–β7), respectively (Baumeister et al., 1998). The proteolytic active sites reside within the central chamber enclosed by the two inner β rings while a small channel formed by the outer α ring, which is primarily closed, restricts access of most native proteins to the catalytic chamber. Appending the RP to the α rings confers ubiquitin- and ATP-dependent protein degradation activity on the 26S proteasome.

The RP consists of 19 different subunits and can be divided into two subcomplexes, the base and the lid (Glickman et al., 1998). The base is composed of six different homologous AAA-ATPase subunits, Rpt1–Rpt6, and three non-ATPase subunits, Rpn1, Rpn2, and Rpn13, although it is also proposed that Rpn13 is not a regular subunit and dynamically interacts with Rpn2 (Hamazaki et al., 2006; Jorgensen et al., 2006; Qiu et al., 2006; Wang and Huang, 2008; Yao et al., 2006). The ATPase subunits are required not only for substrate unfolding with energy liberated from ATP hydrolysis, but also for α ring channel opening exerted by C-termini of Rpt2 and Rpt5 (Gillette et al., 2008; Rabl et al., 2008; Smith et al., 2007), which are prerequisite for threading substrates into the CP. Three of the base subunits, Rpn1, Rpn13, and Rpt5, as well as Rpn10, which is assumed to sit at the interface of the lid and the base, capture ubiquitinated proteins either directly or indirectly. The lid is composed of nine non-ATPase subunits, Rpn3, Rpn5–9, Rpn11–12, and Rpn15 (also called Sem1 in yeast and DSS1 in mammals), where the metalloisopeptidase Rpn11 plays an essential role in deubiquitination of captured substrates (Verma et al., 2002; Yao and Cohen, 2002).

The molecular mechanism involved in the assembly of such an elaborate machine remains a mystery. Recent studies have described in detail the mechanisms of the CP assembly,